In Situ Cyclic Loading of Concrete Pavement Overlays Supported on Geotextile and Asphalt Interlayers: Buchanan County Road D-16

Final Report
February 2022

IOWA STATE UNIVERSITY
Institute for Transportation

National Concrete Pavement Technology Center

CP Tech Center

About the CP Tech Center

The mission of the National Concrete Pavement Technology Center (CP Tech Center) at Iowa State University is to unite key transportation stakeholders around the central goal of advancing concrete pavement technology through research, technology transfer, and technology implementation.

About the Institute for Transportation

The mission of the Institute for Transportation (InTrans) at Iowa State University is to save lives and improve economic vitality through discovery, research innovation, outreach, and the implementation of bold ideas.

Technical Report Documentation Page

1. Report No. InTrans Project 20-741	2. Government Accession No.	3. Recipient's Catalog No.	
4. Title and Subtitle In Situ Cyclic Loading of Concrete Pavement Overlays Supported on Geotextile and Asphalt Interlayers: Buchanan County Road D-16		**5. Report Date** February 2022	
		6. Performing Organization Code	
7. Author(s) David White (orcid.org/0000-0003-0802-1167), Peter Taylor (orcid.org/0000-0002-4030-1727), Pavana Vennapusa (orcid.org/0000-0001-9529-394X), Tom Cackler (orcid.org/0000-0003-4430-4826), and Yifeng Ling (orcid.org/0000-0002-8846-0524)		**8. Performing Organization Report No.** InTrans Project 20-741	
9. Performing Organization Name and Address National Concrete Pavement Technology Center Iowa State University 2711 South Loop Drive, Suite 4700 Ames, IA 50010-8664		**10. Work Unit No. (TRAIS)**	
		11. Contract or Grant No.	
12. Sponsoring Organization Name and Address Technology Transfer Concrete Consortium (TTCC) Transportation Pooled Fund 800 Lincoln Way Ames, IA 50010	Iowa Department of Transportation (lead state) 800 Lincoln Way Ames, IA 50010	**13. Type of Report and Period Covered** Final Report	
		14. Sponsoring Agency Code Also for TPF-5(437)	

15. Supplementary Notes
Visit https://intrans.iastate.edu/ or https://cptechcenter.org/ for color pdfs of this and other research reports.

16. Abstract

Automated plate load tests (APLTs) were conducted on County Road (CR) D-16 in Buchanan County, Iowa, to assess and compare the performance of unbonded concrete overlay test sections with three different geotextile fabric interlayers. The pavement was constructed in 2020. Field testing was performed on the asphaltic cement concrete (ACC) pavement prior to construction and then on the unbonded concrete overlay 2 months after construction and 1 year after construction. Cyclic and static APLTs were performed to assess the composite modulus and permanent deformation.

Test results showed that the permanent deformation decreased by about 50 times after placing the PCC overlay over the ACC, both in sections with and without the geotextile interlayers. The composite resilient modulus values on the overlay increased about 10 times when compared to modulus values on the underlying ACC. Results indicated that the composite resilient modulus was still greater than 200,000 psi be decreased after 1 year along with increased permanent deformation in the control section (no geotextile interlayer). In the sections with a geotextile interlayer, the composite resilient modulus value increased 10% to 30% in two sections and decreased 10% in one section, while the permanent deformations increased by 30% to 60%. Results for the geotextile interlayer sections demonstrated better structural capacity than the control sections and monitoring of the load-deformation response of the pavement structure over time (3, 5, and 10 years after construction) is recommended.

17. Key Words automated plate load tests—geotextile interlayers—overlay structural capacity—PCC overlays		**18. Distribution Statement** No restrictions.	
19. Security Classification (of this report) Unclassified.	**20. Security Classification (of this page)** Unclassified.	**21. No. of Pages** 59	**22. Price** NA

Form DOT F 1700.7 (8-72)   **Reproduction of completed page authorized**

IN SITU CYCLIC LOADING OF CONCRETE PAVEMENT OVERLAYS SUPPORTED ON GEOTEXTILE AND ASPHALT INTERLAYERS: BUCHANAN COUNTY ROAD D-16

Final Report
February 2022

Project Manager
Steven Tritsch, Associate Director
Concrete Pavement Technology Center, Iowa State University

Authors
David White, Peter Taylor, Pavana Vennapusa, Tom Cackler, and Yifeng Ling

A report from
National Concrete Pavement Technology Center
Iowa State University
2711 South Loop Drive, Suite 4700
Ames, IA 50010-8664
Phone: 515-294-8103 / Fax: 515-294-0467
https://cptechcenter.org/

TABLE OF CONTENTS

LIST OF FIGURES

LIST OF TABLES

ACKNOWLEDGMENTS

EXECUTIVE SUMMARY

In this report, results from two phases of work are presented. In the laboratory phase, three different geotextiles were evaluated for their effects on heat transfer, and deflections under load were assessed.

In the field phase, automated plate load tests (APLTs) were conducted on sections of County Road (CR) D-16, which were constructed in 2020, in Buchanan County, Iowa. The field tests were conducted to compare and assess the load-deformation performance of unbonded concrete overlay sections constructed with different geotextile fabric interlayers.

Cyclic and static APLTs were conducted on the existing asphalt cement concrete (ACC) pavement, after constructing the portland cement concrete (PCC) overlay with geotextile interlayers. Testing on the overlay was performed about two months after construction and again one year later. Cyclic APLTs included 1,000 to 2,000 cycles at one selected stress (90 to 100 psi), and static APLTs included an incremental static load test up to 120 psi.

The key findings from the testing and analysis were as follows:

- The amount of energy stored and transferred into a concrete mixture from a geotextile was significantly lower than that from an asphalt layer.

- The composite modulus plots indicated that, even after the concrete started deflecting, the textile was still able to absorb some additional strain. Deflection of the geotextiles was ~0.05 in.

- The composite resilient modulus ($M_{r\text{-comp}}$) values on the existing ACC pavement ranged from 27.7 ksi to 45.1 ksi based on 12 test locations. The values increased in the first 10 to 20 cycles and then remained relatively constant up to 1,000 cycles. The permanent deformation (δ_p) values increased with the number of loading cycles up to 1,000 cycles following a power model trend. At the end of 1,000 cycles, δ_p ranged between 0.19 in. (190 mils) and 0.34 in. (340 mils) at the test locations.

- The backcalculated ACC layer dynamic modulus (corrected for surface temperature to 72°F) at the test locations varied between 76.2 ksi and 140.9 ksi. The base resilient modulus ($M_{r\text{-Base}}$) varied between 14.3 and 32.3 ksi, and subgrade resilient modulus ($M_{r\text{-SG}}$) varied between 16.8 and 29.1 ksi. Results indicated that the $M_{r\text{-comp}}$ values were strongly correlated to the dynamic modulus of the ACC layer ($E^{'}_{AC}$), $M_{r\text{-Base}}$, and $M_{r\text{-SG}}$ values.

- The δ_p values at the end of 1,000 cycles on the PCC overlay (per testing September 23, 2020) ranged between 0.003 in. (3 mils) and 0.007 in. (7 mils) at nominal cyclic stress = 90 psi. In comparison to the existing ACC pavement, the δ_p values on the PCC overlay decreased by about 50 times.

- The δ_p values at the end of 2,000 cycles on the PCC overlay per testing September 1, 2021 ranged between 0.008 in. (8 mils) and 0.011 in. (11 mils), at nominal cyclic stress = 90 psi. The δ_p values (at 1,000 cycles) in all the sections were low (<0.05 in.) but higher than initial testing on September 23, 2020.

- The M_{r-comp} values ranged between 216 ksi and 450 ksi on the PCC overlay per testing September 1, 2021, which represented about a 10 times increase in the modulus after placing the PCC overlay in comparison to the original ACC pavement. The M_{r-comp} values ranged between 184 and 317 ksi on September 1, 2021. The M_{r-comp} values reduced in the control section by 250%, while the M_{r-comp} values increased nominally (10% to 30%) in the white and standard black geotextile sections. The M_{r-comp} value in the thin black geotextile section reduced nominally (10% lower September 1, 2021 compared to September 23, 2020).

- The backcalculated k-value and E_{PCC} comparison for static and cyclic loading cases are presented in this report and is a first of its kind analysis. The current AREA method of backcalculation is based on a static loading case, but the calculation method is widely implemented for dynamic analysis by applying an empirical correction factor to determine a static k-value. This comparison of static and cyclic loading cases to calculate the k-value warrants further detailed analysis.

Recommendations Based on Results

The results presented in this report represent a new method for in situ performance assessment of mechanistic properties of unbonded concrete overlays. Findings showed that the structural capacity of the pavement decreased (as indicated with reduced M_{r-comp} by 250% and increased δ_p by 80%) about one year after initial testing in the control section. The geotextile interlayer section demonstrated suitable performance and perhaps better performance than the control section.

Given these results, the researchers recommend continued monitoring of the changes in the load-deformation response of the pavement structure over time (3, 5, and 10 years after construction). Further, the ride quality of the test sections, i.e., international roughness index (IRI) and pavement condition index (PCI), with and without the geotextile fabric interlayers, should also be documented annually.

Consideration of testing to determine the in situ drainage capacity of the interlayer is also recommended and can be achieved using the core hole permeameter (CHP) test device that was developed as part of a previous Iowa Highway Research Board project (White et al. 2014). A 6-in. diameter core is required for the CHP test.

INTRODUCTION

Nonwoven geotextile materials have been used as the separation layer for unbonded concrete overlays of existing concrete pavements in the US since 2008. However, questions remain regarding the thermal effects of different textiles and their effects on movements of the concrete overlay. This work sought to address some of these questions.

The work conducted in the laboratory phase was aimed at assessing the effects of different geotextiles on the temperature of the concrete overlay and assessing the load deflection behavior of the same materials.

In the field phase, automated plate load tests (APLTs) were conducted on County Road (CR) D-16 in Buchanan County, Iowa, to assess performance of unbonded portland cement concrete (PCC) overlay sections constructed in 2020. The unbonded PCC overlay sections were constructed over an asphalt cement concrete (ACC) layer with three different non-woven geotextile fabric interlayers. Areas without geotextile fabric interlayers served as the control sections. The results documented herein provide a performance assessment of the in situ load-deformation response and composite modulus of the pavement systems.

Traditionally, an ACC interlayer (1 to 2 in. thick) has been used for concrete overlays to act as a bond breaker for stress relief and to reduce reflective cracking. Research efforts are being performed to assess if geotextile fabric can be used as an alternative to the ACC interlayer. In addition to acting as a bond breaker, Lederle et al. (2013) suggested that a geotextile interlayer can improve drainage.

The use of a geotextile fabric interlayer was initiated in the US after positive results in Germany, as noted in a Federal Highway Administration (FHWA) European scan study (Hall et al. 2007). Several field trails have been initiated in the US since 2008 with geotextile fabric as the interlayer in lieu of the ACC interlayer for concrete overlays (Rasmussen and Garber 2009, Wiegand et al. 2010, Fick et al. 2021, Burwell 2014).

A recent study (White and Taylor 2018) documented the first round of APLT results on Poweshiek CR V-18 in Iowa to assess and compare performance of unbonded concrete overlay sections constructed in 2008 and 2009. The APLT results showed that, on average, the composite resilient modulus ($M_{r\text{-}comp}$) was greater and permanent deformation (δ_p) was less in the geotextile sections compared to the ACC layer sections.

Geotextiles have been in use as a separation layer for more than a decade in the US (Cackler et al. 2018), but some questions remain in terms of long-term performance, including:

- How does the geotextile influence vertical deflections in the system?
- Does this tendency change over time?
- Is the risk of slab migration changed?
- Are the geotextile layers effective at providing drainage, and does this change over time?
- Does the risk of cracking change?
- Does the color of the textile affect the thermal effects of the slab?

- Does the thickness of the textile matter?

In this study, a testing program was developed to assess the influences of the different geotextiles in terms of load-deformation response, changes over time, and how the underlaying pavement foundation system affects the performance of the overlay. Recommendations are provided for additional follow-up field testing and analysis to characterize the long-term differences in the mechanistic properties of the concrete overlays with and without the geotextile fabric.

LABORATORY TESTS

The work conducted in the laboratory phase included the following:

- Compare specific heat capacity of three textile samples, and that of an asphalt sample as a control, and tie that to the impacts on concrete layer temperatures
- Measure the temperature rise behind the sample exposed to and infrared lamp to assess how much energy is transferred by the textile
- Measure load deflection plots for bare textiles between metal plattens and between concrete layers

Samples

The three geotextiles evaluated were the same as those used in the field work (see Figure 1 and Table 1).

Figure 1. Edge view of the three geotextile samples evaluated

Table 1. Summary of geotextile products used in this study

Product	Specification	ID	Manufacturer
Standard Black Geotextile	13–15 oz/yd^2	MPBBC1450	Tencate
White Geotextile	13–15 oz/yd^2	Reflectex	Propex
Thin Black Geotextile	5–7 oz/yd^2	Mirafi 160N/12.5/360	Tencate

The concrete test samples were prepared by taking hardened 4x8 in. cylinders and cutting them in half to form 4x4 in. cylinders. These were then placed back into a 4x8 in. mold with a layer of geotextile on them, followed by fresh concrete that was consolidated by rodding. The mixtures used were standard Iowa DOT pavement proportions. Samples were demolded at 24 hours and cured in the fog room until tested.

Tests

Heat Capacity

A spreadsheet was prepared that used the following inputs for a system comprising a concrete layer on a separator layer (asphalt or geotextile) on an (assumed perfectly insulating) base.

- Specific heat capacity of the materials being considered:
  - Concrete – 880 J/K/kg
  - Asphalt – 900 J/K/kg
  - Geotextile – 1800 J/K/kg
- Specific gravity of the materials being considered:
  - Concrete – 2,400 kg/m^3
  - Asphalt – 2,240 kg/m^3
  - Geotextile – 350 kg/m^3
- Layer thickness:
  - Concrete – Typically 6 in. (150 mm)
  - Asphalt – 1 in. (25 mm)
  - Geotextile – 1 or 3.5 mm
- Assumed starting temperature of the separator layer
- Assumed starting temperature of the concrete

The output of the spreadsheet was a rise in the temperature of the concrete layer that could be expected from energy transfer from the hotter separator layer.

Heat Transfer

Heat transfer measurements were recorded by securing a sheet of geotextile across part of a plastic container. Sensors were secured on the top and bottom faces of the geotextile, and temperatures were recorded during exposure to an infrared lamp (see Figure 2).
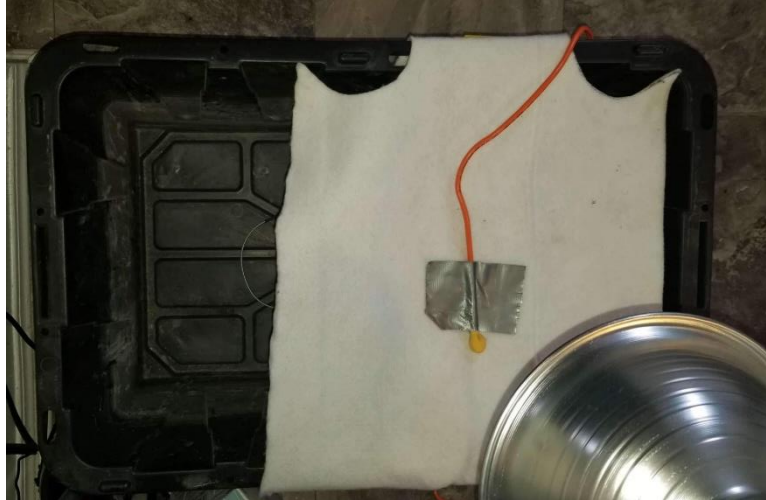
Figure 2. Heat lamp setup

Textile Modulus of Elasticity

Textile-only modulus tests were conducted by placing a single layer textile between plattens, as illustrated in Figure 3.
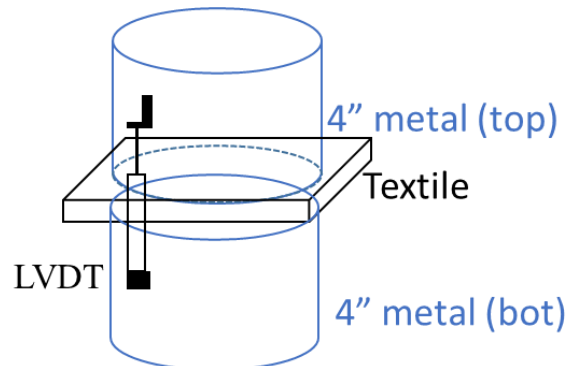
Figure 3. Test configuration for textile-only modulus tests

Loading was applied at the same rate as in ASTM C469, and deflections were recorded using an linear variable differential transformer (LVDT).

Composite Modulus of Elasticity

Modulus tests of the composite samples were conducted in accordance with ASTM C469 (see Figure 4).

Figure 4. Composite modulus samples

Results

Heat Capacity

The calculations indicated that, for a starting state with a separator layer at 120°F and 6 in. of concrete at 90°F, the geotextile may be expected to raise the temperature of the concrete mixture by ~0.3°F, while a 1 in. asphalt layer may be expected to raise the temperature of the concrete mixture by ~8.0°F.

This is largely due to the very low mass of the textile, leading to a small amount of stored heat energy that could be transferred to the concrete.

Heat Transfer

Results of the heat lamp tests are shown in Table 2.

Table 2. Equilibrium temperatures on back and front faces of geotextile exposed to a heat lamp

Geotextile	Exposed face, °F	Shadowed face, °F
Thick Black	111	87
Thick White	102	90
Thin Black	105	104

As expected, the thicker geotextile is shown to be an insulator, and the heat rise is lower in the white material.

Textile Modulus of Elasticity

The load deflection plot for the three textiles is shown in Figure 5.
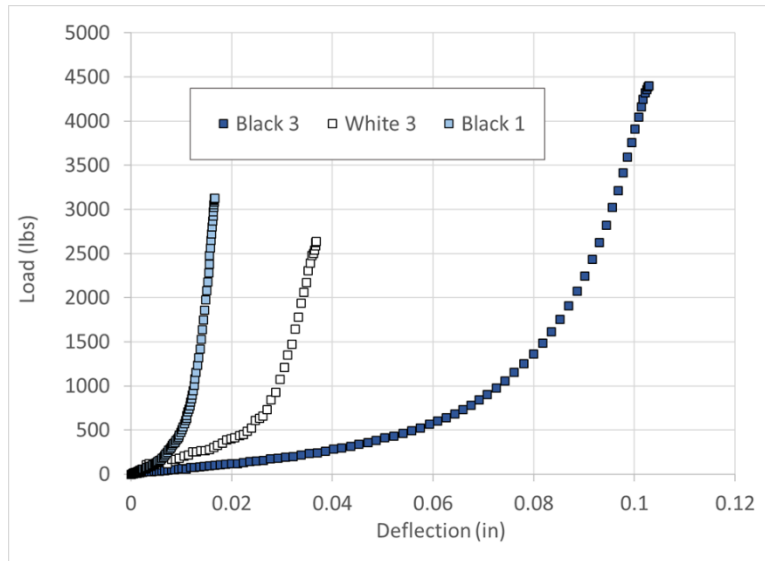
Figure 5. Load deflection plot of geotextiles

The amount of deflection of the textile is consistent with the thickness of the textile (see Figure 1).

Composite Modulus of Elasticity

The load deflection plot for the composite samples is shown in Figure 6.
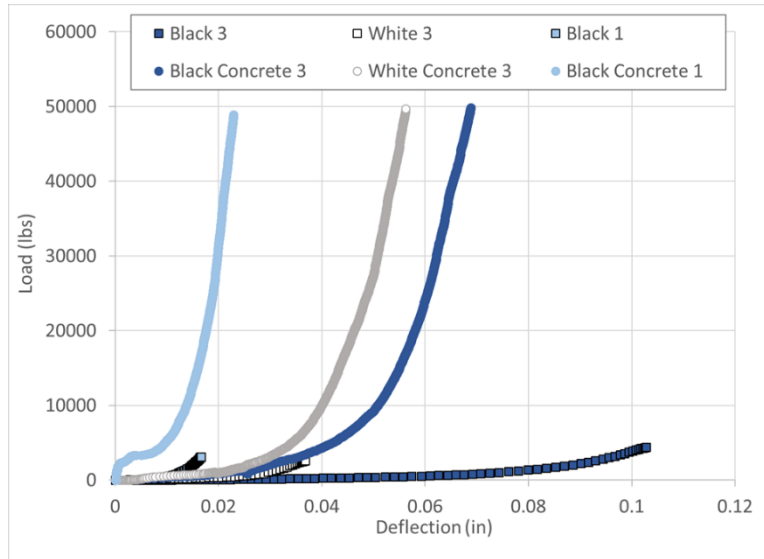
Figure 6. Load deflection plot of composite samples (including the the textile only)

Calculated modulus of elasticity for the composite systems were as follows:

- Thick black – 1,740 ksi
- Thick white – 1,890 ksi
- Thin black – 3,470 ksi

Conclusions

As expected, the data indicate that the amount of energy stored and transferred into a concrete mixture from a geotextile is significantly lower than that from an asphalt layer. A benefit of the thicker geotextiles is that they help insulate the mixture from a hot foundation system.

Both the temperature and stiffness data indicated that the white material was somewhat denser than the black material.

The composite modulus plot indicated that even after the concrete started deflecting, the textile was still able to absorb some additional strain. Deflection of the geotextiles was ~0.05 in.

FIELD TEST SECTIONS

The test sections evaluated in this study were constructed on Buchanan CR D-16 on an existing pavement section with a nominal 12 in. ACC layer over a 6 in. rolled stone (aggregate) base. The unbonded PCC overlay was constructed in July 2020.

Three different non-woven geotextile fabric interlayers were used in the designated test sections. Areas without geotextile fabric interlayers served as the control section. The cross-section details are shown in Figure 7, and an aerial view of the test section limits are shown in Figure 8.
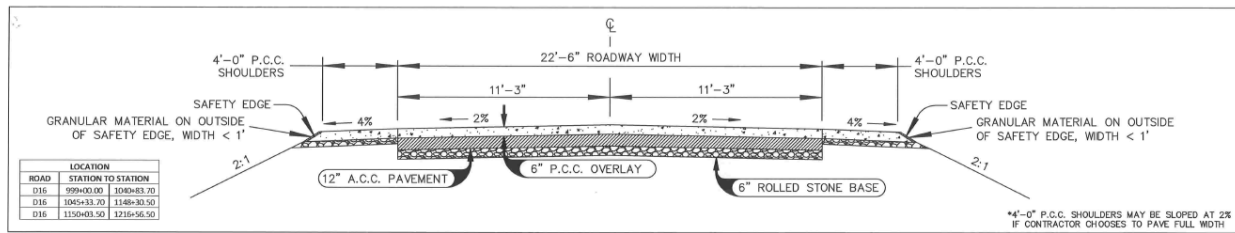
Figure 7. Cross-section of the test sections showing 6 in. PCC overlay on existing 12 in. ACC pavement
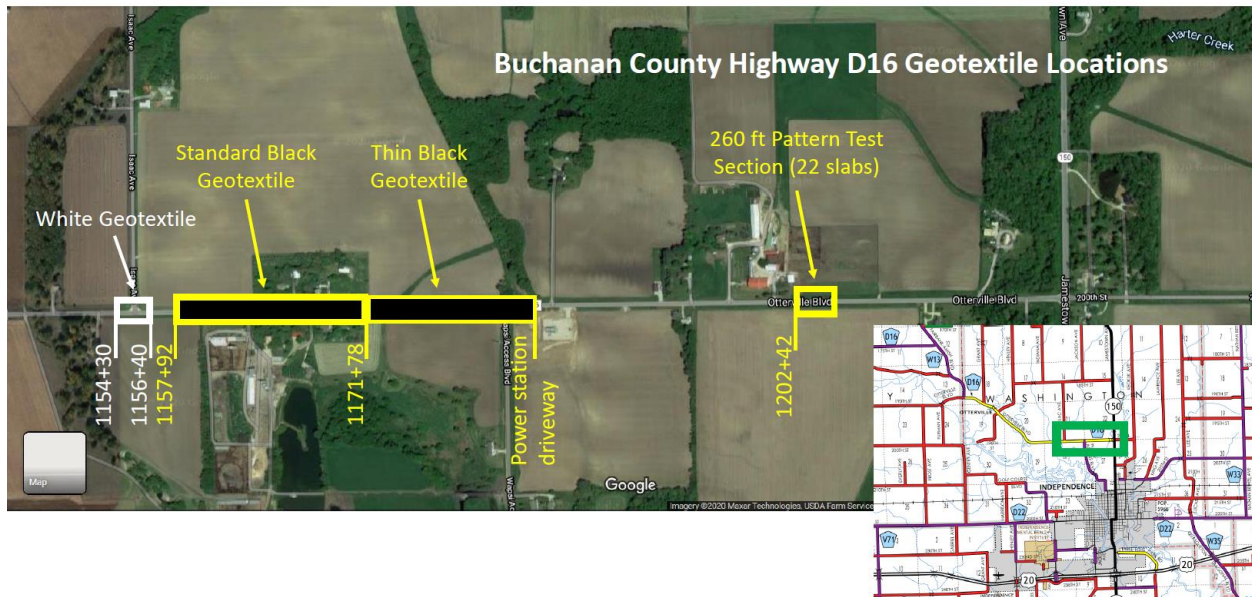
Figure 8. Test sections on Buchanan CR D-16

Table 1 provides a summary of the geotextile products included in this study. Images of the ACC pavement prior to construction and ones taken during the PCC overlay construction and placement of the geotextile interlayers are provided in Figure 9 through Figure 1414.

9

Images taken on July 10, 2020

Figure 9. Existing condition of CR D-16 with ACC surface

Image taken on July 22, 2020, Dan King, Iowa Concrete Paving Association

Figure 10. White and standard black geotextiles placed over existing ACC layer

Image taken on July 22, 2020, Dan King, Iowa Concrete Paving Association

Figure 11. Thin black geotextiles placed over existing ACC pavement

Figure 12. White geotextile placed over existing ACC layer and PCC overlay

Figure13. Control section with no geotextile interlayer placed over ACC layer

Images taken on July 22, 2020, Dan King, Iowa Concrete Paving Association

Figure 14. Surface of PCC overlay

FIELD TESTING METHODS

Automated Plate Load Tests (APLTs)

Ingios Geotechnics, Inc. developed in situ testing and analysis methods and equipment to characterize pavement and its foundation layer mechanistic properties using APLTs. The results are being used to verify pavement and foundation design input parameter values and forecast long-term cyclic loading performance by simulating vehicle loading conditions expected during the service life of a pavement system.

The field testing and evaluation program was designed to characterize the composite resilient modulus and permanent and resilient deformation characteristics on the overlay test sections. Testing involved conducting cyclic APLTs with up to 2,000 cycles using selected cyclic stress levels ranging between 50 psi and 150 psi. A 12 in. diameter flat plate was used for this test program.

The cyclic test process uses a controlled load pulse duration and dwell time (e.g., as simulated in the laboratory using AASHTO TP 62 and AASHTO T 324 methods for asphalt pavements and, as required in the laboratory, AASHTO T 307 resilient modulus test methods for foundation layers) for selected cycle times depending on the field conditions and measurement requirements. The advantage of cyclic tests is that the modulus measurements better represent the field stiffness values. This finding is well documented in the literature and is considered a major short-coming of other testing methods that only apply a few cycles/dynamic load pulses on the pavement layers.

The APLT system has the capability to measure inputs to develop in situ elastic modulus for the PCC layer, dynamic modulus models the ACC layer, and in situ stress-dependent constitutive models for foundation layers (i.e., base and subgrade) as used in AASHTOWare Pavement ME Design (AASHTO 2015). The major advantage of in situ testing is that it does not suffer from the effects of sample preparation, sample size, equipment, or boundary conditions associated with laboratory tests.

Because the APLT test system is automated, the test methods are highly repeatable and reproducible (i.e., no operator bias). Operators input the desired loading conditions (cyclic stress levels, load pulse duration and dwell time, and number of cycles), which are then tightly controlled by the machine feedback control system.

Figure 15 shows the operator station, controls, and on-board display monitor for real-time visualization of results.

Figure 15. APLT equipment setup on the existing ACC layer (top) and after PCC overlay (bottom)

The results of cyclic deformation, permanent deformation, elastic modulus, stiffness, resilient modulus, cyclic stresses, and number of cycles are calculated in real-time and are available for reporting immediately (see illustration of key parameters in Figure).
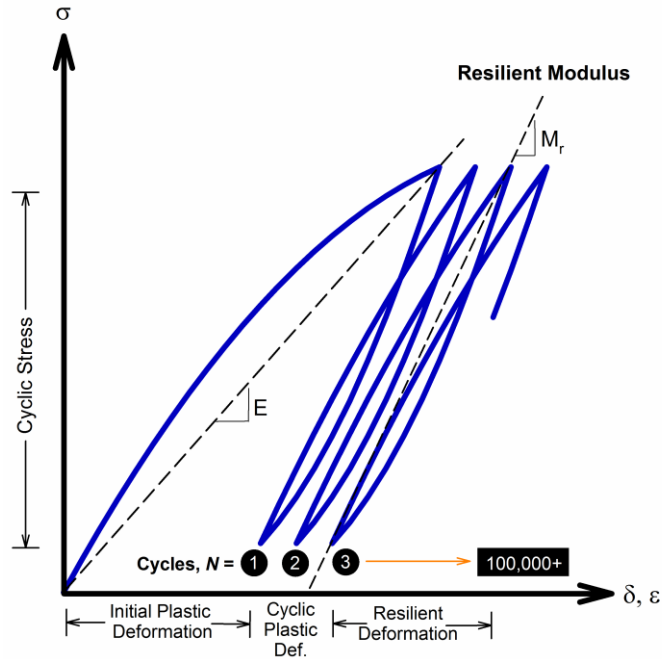
Figure 16. Parameters measured from cyclic APLTs

Testing on ACC Pavement

Cyclic APLTs were performed on the existing ACC pavement to obtain composite and individual layer moduli measurements using a 12 in. diameter plate on the ACC surface and a sensor kit that measures pavement surface deflections at radii of 12 in. (2r), 18 in. (3r), and 24 in. (4r) away from the plate center. An image of the test setup is shown in Figure17.
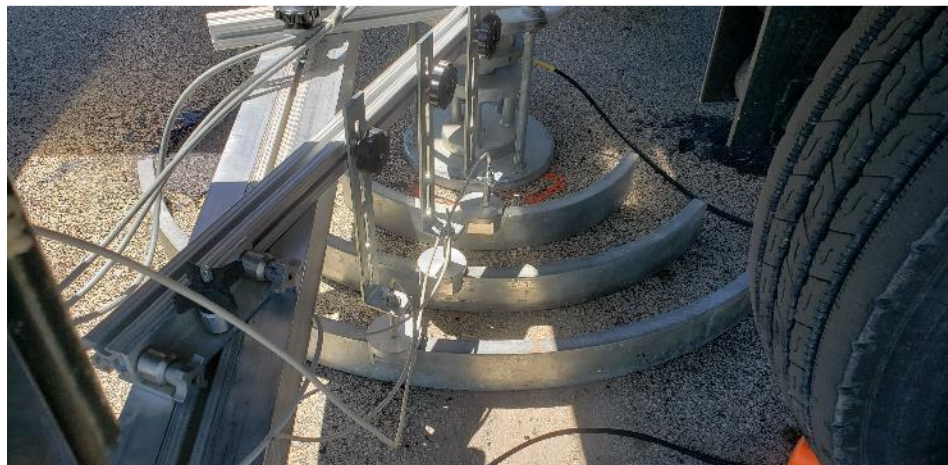
Figure 17. 12 in. diameter plate setup with reference beam for deflection basin measurements on ACC pavement prior to constructing the overlay

The layered analysis calculations are described in the following sections of the report. The following key parameters were assessed from the testing results:

- Composite resilient modulus ($M_{r\text{-comp}}$)
- Dynamic modulus of the ACC layer (E'_{AC})
- Resilient modulus of the underlying foundation layers, base ($M_{r\text{-Base}}$) and subgrade ($M_{r\text{-SG}}$)
- Permanent deformation (δ_p) behavior under cyclic loading

The APLT program on ACC pavement involved a cyclic test with a load pulse time of 0.2 sec. and a dwell (rest) time of 0.8 sec. for 1,000 load cycles at a nominal cyclic stress of 100 psi. The cyclic test was designed to measure the plate rebound deformation and deformation basin parameters (at selected locations) and the permanent deformation (δ_p).

Testing on PCC Overlay

Static and cyclic APLTs were performed on the PCC overlay. The following key parameters were assessed from the test results:

- Composite resilient modulus ($M_{r\text{-comp}}$)
- Modulus of subgrade reaction (k-value)
- Permanent deformation (δ_p) response with accumulated cyclic loading

The APLT program involved a six-step static load test with incremental loading steps applied to a 12 in. diameter rigid loading plate at 10, 20, 40, 60, 80, and 120 psi stress levels with surface deflection basin measurements obtained at r, 2r, 4r, and 6r (r = plate radius). An image of the test setup is shown in Figure 18.

Figure 18. 12 in. diameter plate setup with reference beam for deflection basin measurements on PCC overlay

For reference, about 80 psi contact stress represents the load on a single tire under an 18-kip axle load. The test involved an incremental repeated load step by unloading and re-loading up to 120 psi. The deflection basin and applied stresses were measured for each load step.

Following the static test, a cyclic test with a load pulse time of 0.2 sec. and a dwell (rest) time of 0.8 sec. was performed for 1,000 to 2,000 load cycles at a cyclic stress of about 80 psi. The cyclic test was designed to measure the rebound deformation basin parameters and permanent deformation (δ_p).

Resilient Deformation and Composite Resilient Modulus

In this field study, cyclic APLTs were performed to obtain composite resilient moduli measurements ($M_{r\text{-}comp}$) and resilient deformation (δ_r) values using the 12 in. diameter plate on the PCC overlay surface.

The composite resilient moduli ($M_{r\text{-}comp}$) values provide a measure of the composite responses of the pavement layer and the supporting layers under dynamic loading. This value can be used to quickly compare the support conditions between test points. The $M_{r\text{-}comp}$ values from APLTs were calculated using the modified Boussinesq's elastic half space solution equation, which is shown in Equation 1.

$$M_{r-comp} = \frac{(1-v^2)\sigma_0 a}{\delta_r} \times f \qquad (1)$$

where, M_{r-comp} = in situ composite resilient modulus, δ_r = the resilient deflection of the plate during the unloading portion of the cycle (determined as the average of three measurements along the plate edge, i.e., at a radial distance $r' = r$), v = Poisson ratio (assumed as 0.4), σ_o = cyclic stress, a = radius of the plate, and f = shape factor selected as 8/3.

Permanent Deformation

Within the pavement profile, permanent deformations (δ_p) accumulate with cyclic loading from the following: plastic shear strains, compaction (removal of air void space), and consolidation (removal of water in void space) during loading. δ_p of the loading plate was measured during cyclic APLTs. From the number of load cycles (N) versus the δ_p plot, a deformation prediction model can be calculated from the various power and logarithmic functions. A power model was selected to represent the permanent deformation versus the number of cycles, as shown in Equation 2.

$$\delta_p = CN^d \qquad (2)$$

where, coefficient C is the plastic deformation after the first cycle of repeated loading, and [d] is the scaling exponent. Using the power relationship parameters, the number of cycles required to achieve a near-linear elastic state (change in δ_p [$\Delta\delta_p$] of 1E-6 in./cycle), represented as N*, is calculated for each test to forecast and compare the performance of different sections.

Monismith et al. (1975) described a similar power model relationship for relating permanent strain to cycle loadings for repeated triaxial laboratory testing. It is expected that regression coefficients, C and d, depend on the material and stress conditions.

Layered Analysis Calculations on ACC Pavements

Layered analysis calculations on ACC pavements were performed using advanced proprietary software (COMP-Score APLT-BACK) developed in March 2017 by Ingios Geotechnics, Inc. The program was developed using a numerical algorithm to solve an extended formulation of the linear-elastic analysis theory. The pavement layers are idealized as a multi-layered linear elastic half-space. The algorithm employs piecewise linear integration, an automatic integration step size, and gradation in performing the numerical inversion. The program uses an optimization method to match the measured deflection basin with a predicted deflection basin from a static model and iteratively modifies the layer moduli values. This procedure is referred to as the backcalculation method, and the iterations are continued until a selected minimum root mean squared (RMS) value is obtained between the measured and calculated deflection values.

Other backcalculation software programs normally model loading on a flexible plate with a uniform stress distribution. The assumption of a uniform stress distribution is not accurate because of the rigidity of the plate. The APLT-BACK program addresses this issue by modeling the loading on a rigid (or semi-rigid) plate with constant deformation beneath the plate. This feature is considered an advancement over other methods (e.g., BAKFAA from the FAA 2007). Comparison of normalized plate deformations and deflection basins under flexible and rigid plates resting on an elastic halfspace is provided for illustration of the differences in Figure19.
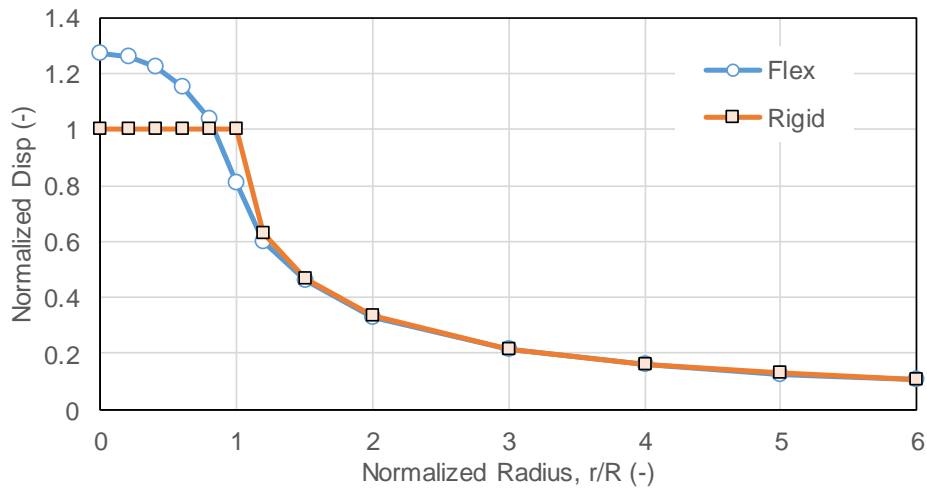
Figure 19. Comparison of plate deformations and deflection basin with rigid and flexible plates resting on an elastic halfspace

The practical consequence of assuming the plate is flexible with constant stress distribution is that the predicted surface layer moduli values are over-estimated. The rigid plate analysis is expected to provide more realistic moduli values for the surface layer.

Deflection basins calculated for four different combinations of a three-layered profile (bottom layer assumed as semi-infinite halfspace) using the APLT-BACK program with rigid and flexible plate configurations is provided in Figure20.
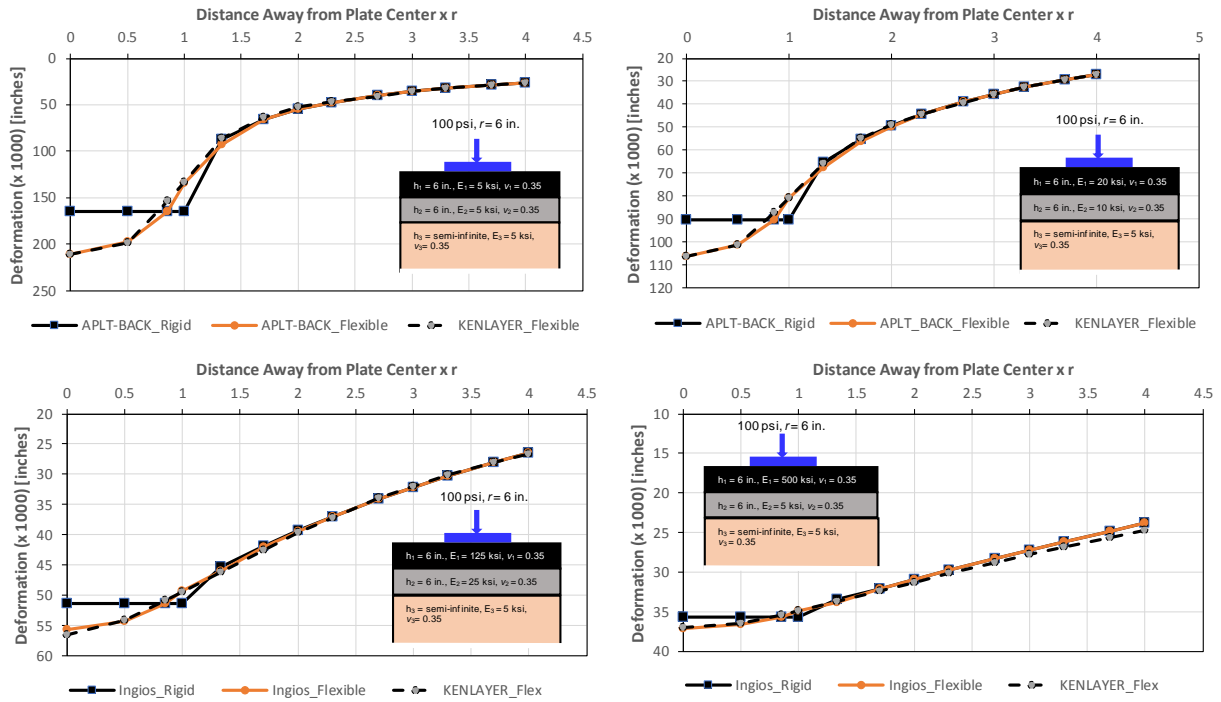
Figure 20. Plate deformations and deflection basins calculated with rigid and flexible plate configurations on three-layered profiles using APLT-BACK and Kenlayer layered analysis program

The flexible plate configuration results from APLT-BACK are compared with those from the Kenlayer layered analysis program, which was developed by Yang H. Huang with the University of Kentucky (Huang 2004). The deformations calculated from Kenlayer analysis and APLT-BACK flexible plate analysis show a match with R^2 close to 1 in a linear regression analysis and all the points falling near the 1:1 line (Figure21), thus validating the APLT-BACK program analysis.
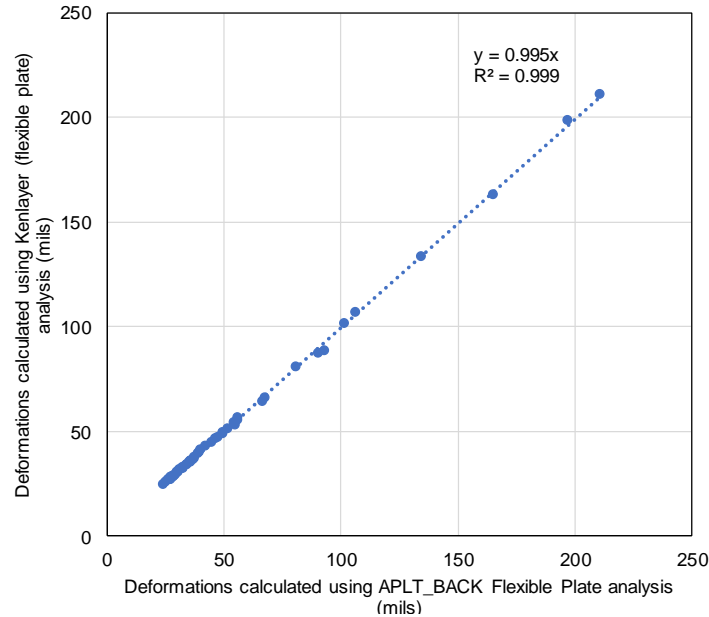
Figure 21. Validation of deformations calculated from APLT-BACK flexible plate analysis with Kenlayer flexible plate analysis

The APLT-BACK program requires the following as inputs: pavement and foundation layer thicknesses, applied load, deflection basin measurements, seed moduli values for each layer, and Poisson's ratio of each layer.

In this study, the surface layer thickness was measured by drilling a hole through the pavement layer, and the underlying base layer thickness was interpreted from the dynamic cone penetrometer penetration resistance profiles. The applied load was measured by the APLT results using a calibrated load cell. A brief description of how the remaining input parameters are obtained/selected is summarized in the following subsections.

Deflection Basin Measurements

The deflection basin measurements were obtained by measuring resilient (rebound) deflections at radii of 12 in. (2r), 18 in. (3r), and 24 in. (4r) away from the plate center. The layered analysis measurement sensor kit provided average resilient deflections measured over one-third of the circumference of a circle at the selected radii. This method was designed to improve upon practices that use point measurements, which are often variable from point-to-point, particularly for unbound aggregate materials.

Like the loading plate representing an integrated response of the material under the plate, the deflection basin circumference bars were designed to represent an integrated deflection basis response over a length of one-third the circumference.

Seed Moduli Values

In this study, the pavement layer structure was modeled as a three-layer system, with an underlying subgrade layer that is homogenous and has semi-infinite depth (no stiff/rigid layer or bedrock at depth). The seed moduli value for the AC layer was 250,000 psi.

The moduli values for the subgrade layer were calculated using Equation 3, as suggested by AASHTO (1993).

$$M_{r-SG} = \frac{(1-\nu^2) \cdot P}{\pi \cdot r' \cdot \delta_{r,r'}}$$

(3)

where, M_{r-SG} is the in situ subgrade resilient modulus (psi), $\delta_{r,r'}$ is the resilient deflection (in.) during the unloading portion of the cycle at $r' = 2r$ or $3r$ or $4r$ away from plate center, ν is the Poisson's ratio (assumed, herein as 0.40), and P is the cyclic load (lbs.).

AASHTO (1993) suggests that r' must be far enough away that it provides a good estimate of the subgrade modulus, independent of the effects of any layers above but also close enough that it does not result in too small of a value. A graphical solution is provided in AASHTO (1993) to estimate the minimum radial distance based on an assumed effective modulus of all layers above the subgrade and the $\delta_r=0$ value.

Ullidtz (1987) indicated if the modulus values are plotted against radial distance, r, in linear elastic materials such as sands and gravels, the modulus values decrease with increasing distance and then level off after a certain distance. The distance at which the modulus values level off can be used as r' in Equation 3.

In some cases, the modulus values decrease and then increase with distance. Such conditions represent either soils with moderate to high moduli with poor drainage at the top of the subgrade or soft soils with low moduli. In those cases, the distance where the modulus is low can be used as r' in Equation 3.

In this study, $r' = 2r$, $3r$, or $4r$, depending on which produced the lowest value, was used to determine the moduli value for M_{r-SG}. The moduli value of the subgrade was then fixed and was not used in the iteration process. Only the moduli values of the asphalt and the foundation layers were modified in the iteration process when matching the predicted and measured deflection basin measurements.

Interface Bonding

The assumption of a fully-bonded versus an un-bonded condition between the pavement and underlying base layer has a significant impact on the backcalculated granular base layer moduli values. A fully-bonded condition results in lower base layer moduli values compared to a no-

bonded condition at the hot-mixed asphalt (HMA) and granular base layer interface (Romanoschi and Metcalf 2003).

Past research has shown that the bonding strength within the AC layers (wearing and base courses) changes as a function of the pavement temperature and the applied normal stress. Several researchers have concluded that, as temperature increases, the interface bonding strength decreases (Sholar et al. 2002, Tandon and Deysarkar 2005, Canestrari and Santagata 2005, West et al. 2005). The reason for a decrease in bond strength is that, at higher temperatures, the tack coat loses its adhesion, and the shear resistance comes primarily from the layer surface roughness (West et al. 2005). This implies that the shear resistance at layer interfaces in the field are likely to be lowest on hot days.

At the time of this report, the authors were not aware of any studies that document the bonding strength between the AC and granular base course layers as a function of pavement temperature. Based on past research findings and the authors' experience with back-calculation analysis, it was assumed in this study that the AC and the granular base layer interface are fully bonded. This assumption provides the most conservative value for granular base layer moduli values, and it does not affect the AC layer or the underlying subgrade layer moduli values.

Temperature Corrections for AC Layer Modulus

The temperature of the AC surface layer has a significant influence on the plate deformation values because of the temperature-dependent nature of the HMA mixtures (PCS/Law Engineering 1993). Many have proposed empirical equations/correction factors to correct the moduli values or the deflection values to a standard reference temperature of 68°F to 72°F (AASHTO 1986, AASHTO 1993, Appea 2003, Baltzer and Jansen 1994, Chang et al. 2002, Chen et al. 2000, Johnson and Baus 1992, Kim et al. 1995, Lukanen et al. 2000, PCS/Law Engineering 1993, Stubstad et al. 1994, Ullidtz and Peattie 1982, Ullidtz 1987).

The corrections in AASHTO (1986), AASHTO (1993), and PCS/Law Engineering (1993) are provided as graphs, while empirical equations are provided in the remaining references cited above. The graphs provided in PCS/Law Engineering (1993) and AASHTO (1993) are shown as a function of the pavement layer thickness. The correction graphs provided in AASHTO (1986) are not a function of pavement thickness. Most of the empirical correction models are adjusted to a single reference temperature. Chen et al. (2000) provided an equation that provides the flexibility to normalize to any reference temperature.

As referenced in the Minnesota DOT (MnDOT) TONN program, the temperature correction equation developed by Lukanen et al. (2000) was used in this study to correct the asphalt layer moduli values to a reference temperature of 72°F (22°C):

$$E_{ref} = E_{test} \times 10^{slope(T_{ref} - T_{test})}$$

(4)

where, E_{ref} = AC layer moduli at reference temperature (22°C or 72°F), E_{test} = AC layer moduli computed at the field temperature, T_{ref} = reference temperature (in °C), T_{test} = in situ temperature at the time of the test, and slope = -0.020 (as suggested by Bly et al. 2011 for use in the TONN program).

In the TONN program that MnDOT currently uses for falling weight deflectometer (FWD) data analysis, in situ AC layer temperature is calculated using the BELLS3 model. Use of the BELLS models, BELLS2 and BELLS3, to predict the mid-depth temperature is described in Lukanen et al. (2000).

The BELLS2 model is used where the measurements are taken over a longer time (>3 min.) and shading affects the surface layer temperature. The BELLS3 model is used where the measurements are taken over a shorter time. The TONN program uses the BELLS3 model because the program was designed for routine testing where the testing time is relatively short.

In this study, the mid-depth pavement temperature was calculated using the BELLS2 model and was also directly measured in accordance with the AASHTO (1986) procedure for comparison. The BELLS2 model was selected over BELLS3 because tests were performed over a longer time (>15 min.) at each test location.

The procedure to directly measure the in situ measurement of the AC layer temperature is provided in AASHTO (1986) Appendix L. The procedure involves measuring temperature at a minimum of three depths within the AC layer—near the surface, mid depth, and near the bottom of the layer—and calculating the average.

The BELLS2 model is provided in Equation 5:

$$T_d = 2.78 + 0.912T_s + \left(\log_{10}(h_d) - 1.25\right) \times \left(-0.428 \times T_s + 0.553T_{1-day} + 2.63 \times \sin(h_{r18} - 15.5)\right)$$
$$+ 0.027T_s \times \sin(h_{r18} - 13.5)$$

(5)

where, T_s = surface temperature in °C, h_{r18} = time of the day with a 24-hour clock, but calculated using an 18-hour temperature rise-and-fall time cycle, as described in Lukanen et al. (2000), h_d = distance below the surface where the temperature is to be calculated in millimeters ($_d$), and T_{1-day} = average air temperature of the previous day in degrees Celsius.

Lukanen et al. (2000) noted that, when using the sine (hr_{18} - 15.5) (decimal) function, only times from 11:00 to 05:00 hours are to be used. If the actual time is not within this time range, the sine function be calculated as if the time was 11:00 hours (where the sine = -1). If the time is between midnight and 05:00 hours, 24 must be added to the actual (decimal) time. When using the $\sin(hr_{18}$ - 13.5) (decimal) function, only times from 09:00 to 03:00 hours are used. If the actual time is not within this time range, the sine function is calculated as if the time is 09:00 hours (where the sine = -1). If the time is between midnight and 03:00 hours, 24 must be added to the actual (decimal) time. An EXCEL spreadsheet has been developed and validated using the

example data provided in Lukanen et al. (2000) to solve the BELLS2 equations and was used in this study.

The average one-day temperatures of the test area were obtained from the temperature readings reported at the Waterloo Regional Airport weather station (Source: https://www.wunderground.com/history/daily/us/ia/waterloo/KALO).

Correction for Effect of Foundation Saturation

Pavement design parameters are typically assumed in a saturated state to represent the worst-case scenario, while the foundation materials were not saturated at the time of testing in the field. AASHTO T 222-81 (2012) recommends conducting odometer tests on subgrade layer samples obtained from the field in saturated and unsaturated conditions to determine the correction factors ($F_{Saturation}$) for k values using Equation 6.

$$F_{Saturation} = \frac{D}{D_s} + \frac{h}{75}\left(1 - \frac{D}{D_s}\right) \tag{6}$$

where D = deformation of odometer sample at in situ moisture content under a unit load of 10 psi (in.), D_s = deformation of saturated odometer sample under a unit load of 10 psi (in.), and h = thickness of base course material (in.). This equation was originally developed by the U.S. Army Corps of Engineers (1995). Barker and Alexander (2012) indicated $F_{Saturation}$ = 0.6 and 0.8 for tests conducted on clays and silts, respectively.

Determining saturation correction factors was beyond the scope of this study, and, therefore, no correction factors were applied to the $M_{r\text{-}Base}$ or $M_{r\text{-}SG}$ values.

Backcalculation Analysis on PCC Overlay

APLT data analysis on the PCC overlay was analyzed as a rigid pavement structure with the underlying ACC layer as a stabilized base layer (Smith et al. 2017).

The static plate load test results were analyzed to determine the pavement foundation k-value and the elastic modulus of the PCC (E_{PCC}) layer using the AREA factor method or the outer AERA method described in AASHTO (1993). The outer AREA factor used in this analysis uses the deflection basin sensor measurements obtained at 4r and 6r, along with normalizing deformations at the 2r position (Smith et al. 2017). The outer AREA method is referred to as the A_3 method (Hall et al. 1997).

Using the A_3 method, the radius of relative stiffness (L_{est}) is calculated. Then L_{est} values are corrected for a finite slab size (assumed as 12 ft for this project) to calculate the adjusted L (L_{adj}), and then the k-value and the E_{PCC} values are determined. The calculation procedure is described in detail by Hall et al. (1997), and corrections for finite slab size are provided by Crovetti (1994).

Herein, the results are presented for incremental stress levels applied for both the first and the second loading cycles. Results from the second loading cycle at 80 psi applied stress are highlighted in the data sheet.

Plate and pavement deformation measurements were monitored for each of the 1,000 to 2,000 loading cycles. Accumulated permanent deformation (δ_p) results were discussed as described previously in this report.

For comparison, the cyclic deflection basin results were used to calculate k-value and E_{PCC} using the same A_3 procedure for the static plate loading case. The k-values calculated from cyclic plate load test results are dynamic measurements and normally divided by an empirical factor 2, per AASHTO (1993), to convert dynamic k-values to static k-values. The comparison values are summarized in each of the data sheets.

Dynamic Cone Penetrometer

DCP tests were performed in accordance with ASTM D6951-03, Standard Test Method for Use of the Dynamic Cone Penetrometer in Shallow Pavement Applications, by drilling a 0.75 in. diameter hole in the pavement down to the bottom of the AC layer and testing the foundation layers. The tests involved dropping a 17.6 lb hammer from a height of 22.6 in. and measuring the resulting penetration depth. A 30 in. penetrating rod was used. California bearing ratio (CBR) values were determined using Equation 7 or 8, whichever was appropriate:

$$CBR(\%) = \frac{292}{DPI^{1.12}} \text{ for all materials except CL soils with CBR<10} \tag{7}$$

$$CBR(\%) = 1/(0.017019 \times DPI)^2 \text{ for CL soils with CBR<10} \tag{8}$$

where, the dynamic penetration index (DPI) is in units of mm/blow.

In this study, the subgrades beneath the aggregate base materials were assumed as CL soils.

FIELD RESULTS AND ANALYSIS

Cyclic APLTs were performed on July 10, 2020 on the existing ACC pavement at 10 locations, as summarized in Table 3.

Table 3. Summary of test point locations on existing ACC pavement prior to PCC overlay (July 10, 2021)

Test Point Number	Station No.	Notes
C-1	1120+34	
C-2	1123+94	
C-3	1125+70	1,000 cycle APLT and DCP performed. Test on ACC layer in control section where no geotextile was placed during overlay construction as interlayer.
WF-1	1135+57	
WF-2	1138+52	
WF-3	1140+47	
BL-1	1157+55	1,000 cycle APLT and DCP performed. Test on ACC layer in control section where white geotextile was placed during overlay construction as interlayer.
BL-2	1162+00	1,000 cycle APLT and DCP performed. Test on ACC layer in control section where standard black geotextile was placed during overlay construction as interlayer.
BL-3	1166+00	
BH-1	1172+00	
BH-2	1174+00	1,000 cycle APLT and DCP performed. Test on ACC layer in control section where thin black geotextile was placed during overlay construction as interlayer.
BH-3	1176+00	

At that time, a DCP test was also performed at selected test locations. The PCC overlay was constructed later in July 2020. Static and cyclic APLTs were performed on September 23, 2020, as summarized in Table 4.

Table 4. Summary of test point locations on PCC overlay (September 23, 2020)

Test Point Number	Station No.	Geotextile Interlayer	Notes
PT1	1154+00	None (Control)	
PT2	1140+47		
PT3	1156+50	White	
PT4	1155+50		1,000 cycle APLT followed by static APLT at each test location
PT5	1162+00	Standard Black	
PT6	1166+00		
PT7	1174+00	Thin Black	
PT8	1176+00		

Static and cyclic APLTs were repeated in the same sections about one year after construction on September 1, 2021, as summarized in Table 5.

Table 5. Summary of test point locations on PCC overlay (September 1, 2021)

Test Point Number	Station No.	Geotextile Interlayer	Notes
PT1	1140+47	None (Control)	
PT4	1156+35	White	2,000 cycle APLT followed by static APLT at each test location
PT5	1162+00	Standard Black	
PT7	1175+00	Thin Black	

Individual test data sheets are provided for each APLT and DCP test and are organized in Appendices A through F.

APLT Results and Analysis

Cyclic APLT results on the existing ACC layer are summarized in Table 6.

Table 6. Summary of test results on existing ACC pavement (July 10, 2021)

Test Point Number	Station No.	Section	$M_{r\text{-comp}}$ (ksi)	E'_{AC} (ksi)	$M_{r\text{-Base}}$ (ksi)	$M_{r\text{-SG}}$ (ksi)	δ_p at 1,000 cycles (in.)
C-1	1120+34		41.0	—*	—*	—*	0.24
C-2	1123+94		29.6	76.6	14.3	16.8	0.25
C-3	1125+70	Control	27.7	—*	—*	—*	0.27
WF-1	1135+57		34.9	—*	—*	—*	0.27
WF-2	1138+52		47.2	140.9	29.2	24.9	0.21
WF-3	1140+47		41.0	—*	—*	—*	0.24
BL-1	1157+55	White Geotextile	40.6	—*	—*	—*	0.19
BL-2	1162+00		40.6	104.6	32.3	29.1	0.19
BL-3	1166+00	Standard Black	43.9	—*	—*	—*	0.14
BH-1	1172+00		30.8	—*	—*	—*	0.34
BH-2	1174+00	Thin Black	30.8	76.2	27.4	22.6	0.34
BH-3	1176+00		45.1	—*	—*	—*	0.30

*No deflection basin measurements obtained

These tests were performed to assess the structural capacity of the existing layer prior to placing the PCC overlay. The individual test data sheets are included in Appendix A. The surface condition at the time of testing showed distresses with transverse and longitudinal cracking (Figure 9 and Figure22).

Image taken on July10, 2020

Figure 22. Surface indent after 1,000 cycles at test loctaion C-1 at Sta. 1120+34

The permanent deformation (δ_p), and $M_{r\text{-comp}}$ values for 1,000 cycles (at nominal cyclic stress = 100 psi) at test locations between Sta. 1135+57 and 1176+00 are shown in Figure23.
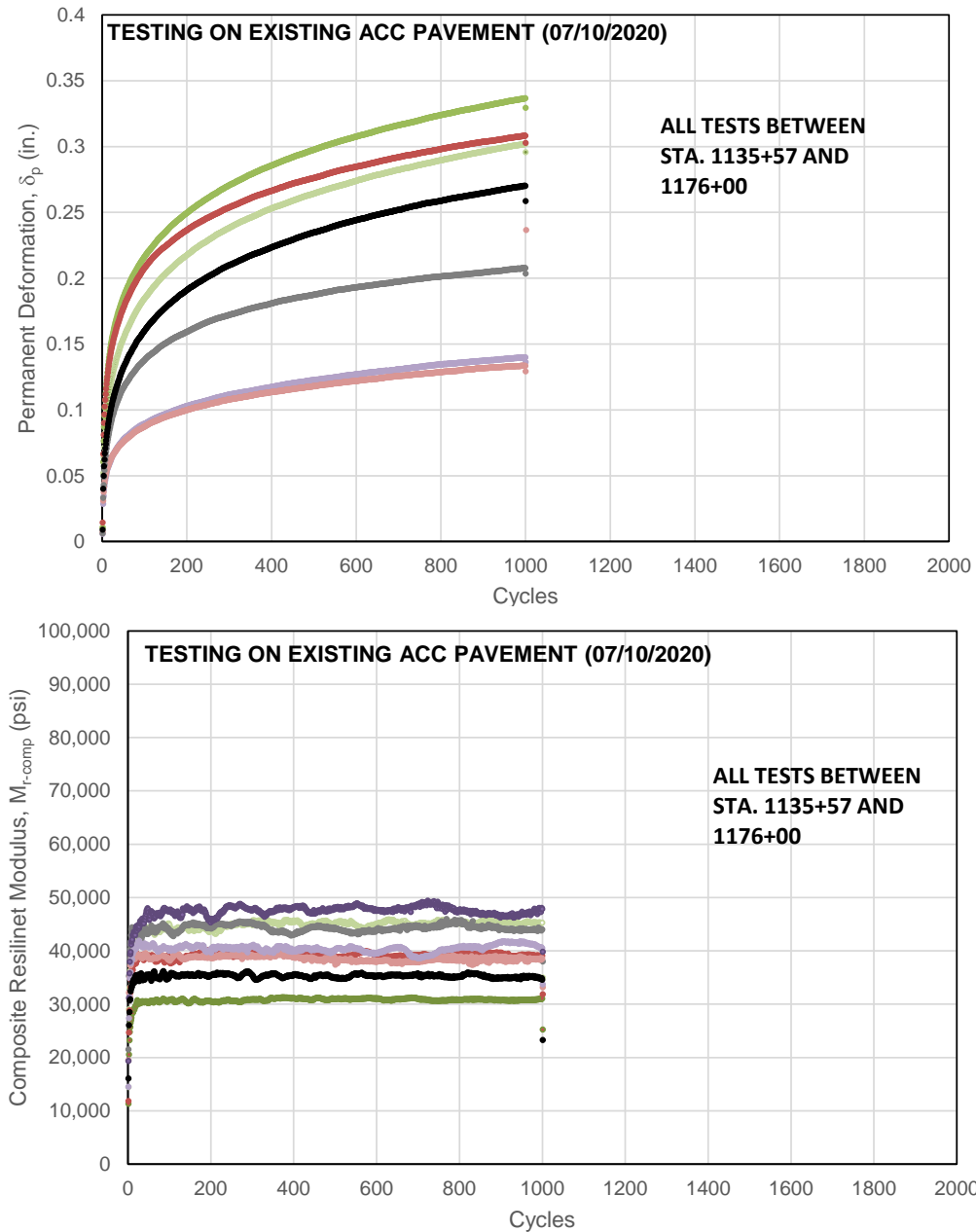
Figure 23. Cyclic APLT results on existing ACC pavement layer – permanent deformation (δ_p) at end of and $M_{r\text{-comp}}$ test

The $M_{r\text{-comp}}$ values of the existing pavement structure varied between 27.7 ksi and 45.1 ksi between Sta. 1120+34 and 1176+00 at the 12 test locations. The $M_{r\text{-comp}}$ values increased in the first 10 to 20 cycles and then remained relatively constant up to 1,000 cycles. The δ_p values increased with the number of loading cycles. δ_p at the end of 1,000 cycles ranged between 0.19 in. and 0.34 in. at the test locations. A permanent indentation of the loading plate was visible at the completion of the test, which was an indication that the test provided an accelerated assessment of performance resulting in permanent deformation.

Deflection basin measurements were obtained at four of the test locations to back calculate the ACC layer and the underlying foundation layer modulus values. The thickness of the ACC layer was measured at each of the test location using the hole drilled in the pavement for the DCP test. The DCP penetration resistance and CBR profiles were assessed for the underlying base layer thickness. DCP test results are provided in Appendix B.

The backcalculated ACC layer dynamic modulus (corrected for surface temperature to 72°F) at the test locations varied between 76.2 ksi and 140.9 ksi, the resilient modulus of the base layer (M_{r-Base}) varied between 14.3 and 32.3 ksi, and the underlying subgrade layer resilient modulus (M_{r-SG}) varied between 16.8 and 29.1 ksi. Results indicated that the M_{r-comp} values strongly correlated to the E'_{AC}, M_{r-Base}, and M_{r-SG} values.

Cyclic and static APLT results about two months after the PCC overlay was constructed (September 23, 2020) are summarized in Table 7 and Table 8, respectively, with two tests in each of the identified geotextile interlayer sections and a control section.

Table 7. Summary of test results on PCC overlay from cyclic APLT (September 23, 2020)

Test Point Number	Station No.	Geotextile Interlayer	M_{r-comp} (ksi)	δ_p at 1,000 cycles (in.)	k-value	E_{PCC} (ksi)
PT1	1154+00	None (Control)	238.1	0.006	304	2,868
PT2	1140+47		450.2	0.006	307	11,973
PT3	1156+50	White	370.1	0.007	219	11,974
PT4	1155+50		254.6	0.005	220	4,943
PT5	1162+00	Standard Black	216.5	0.006	226	3,316
PT6	1166+00		361.3	0.003	320	6,811
PT7	1174+00	Thin Black	313.7	0.005	338	4,633
PT8	1176+00		316.2	0.004	447	3,364

Table 8. Summary of test results on PCC overlay from static APLT (September 23, 2020)

Test Point Number	Station No.	Geotextile Interlayer	k-value	E_{PCC} (ksi)
PT1	1154+00	None (Control)	351	4,459
PT2	1140+47		378	22,622
PT3	1156+50	White	310	18,983
PT4	1155+50		395	5,945
PT5	1162+00	Standard Black	276	6,348
PT6	1166+00		335	11,633
PT7	1174+00	Thin Black	336	6,714
PT8	1176+00		423	5,516

The tests were repeated at or near one of the test locations in each of the sections about one year after the overlay was constructed (September 1, 2021), and the results are summarized in Table 9 and Table 10.

Table 9. Summary of test results on PCC overlay from cyclic APLT (September 1, 2021)

Test Point Number	Station No.	Geotextile Interlayer	$M_{r\text{-comp}}$ (ksi)	δ_p at 2,000 cycles (in.)	k-value	E_{PCC} (ksi)
PT1	1140+47	None (Control)	183.8	0.011	247	1,744
PT2	1156+50	White	316.6	0.008	256	6,024
PT3	1162+00	Standard Black	275.3	0.009	267	5,034
PT7	1175+00	Thin Black	272.2	0.009	318	3,671

Table 10. Summary of test results on PCC overlay from static APLT (September 1, 2021)

Test Point Number	Station No.	Geotextile Interlayer	k-value	E_{PCC} (ksi)
PT1	1140+47	None (Control)	477	3,156
PT2	1156+50	White	971	6,823
PT3	1162+00	Standard Black	369	7,069
PT7	1175+00	Thin Black	397	3,865

The individual test data sheets are included in Appendices C through F.

The cyclic APLTs performed on September 23, 2020 involved 1,000 cycle tests. On September 1, 2021, the number of cycles were extended to 2,000 based on the results showing the increasing δ_p and decreasing $M_{r\text{-}comp}$ trend (increasing rebound values) at the test locations.

Figure 2424 compares δ_p results from September 23, 2020 and September 1, 2021 cyclic APLTs performed in the different sections.
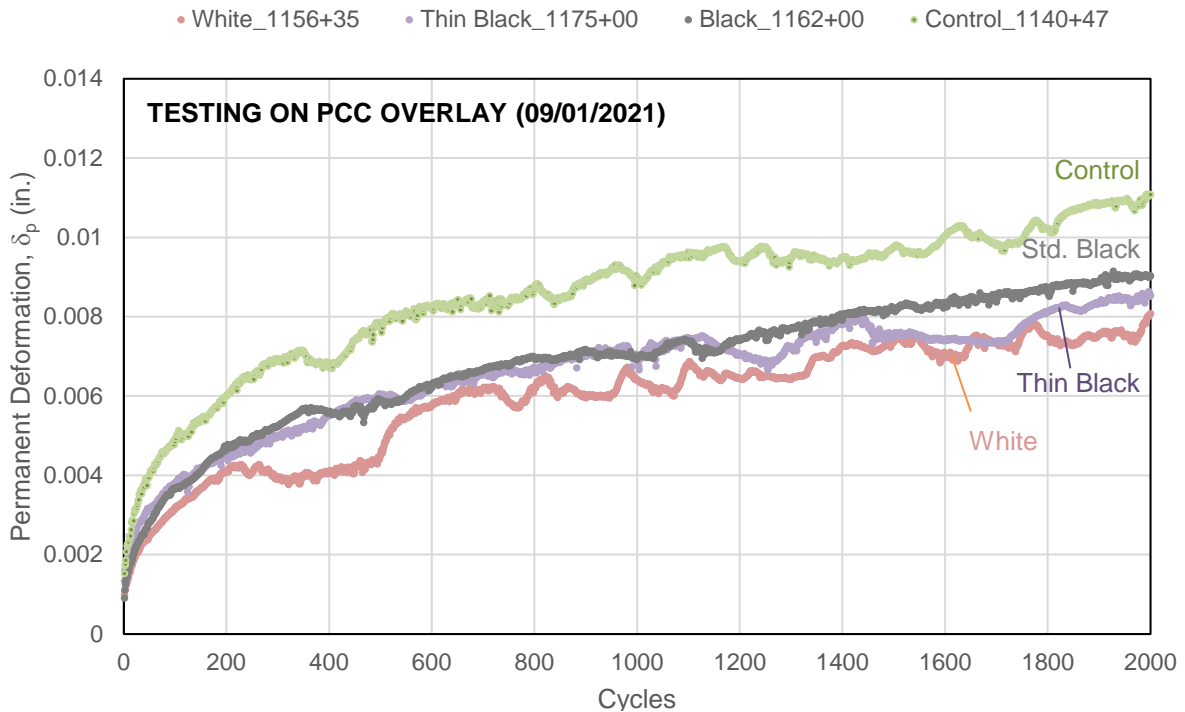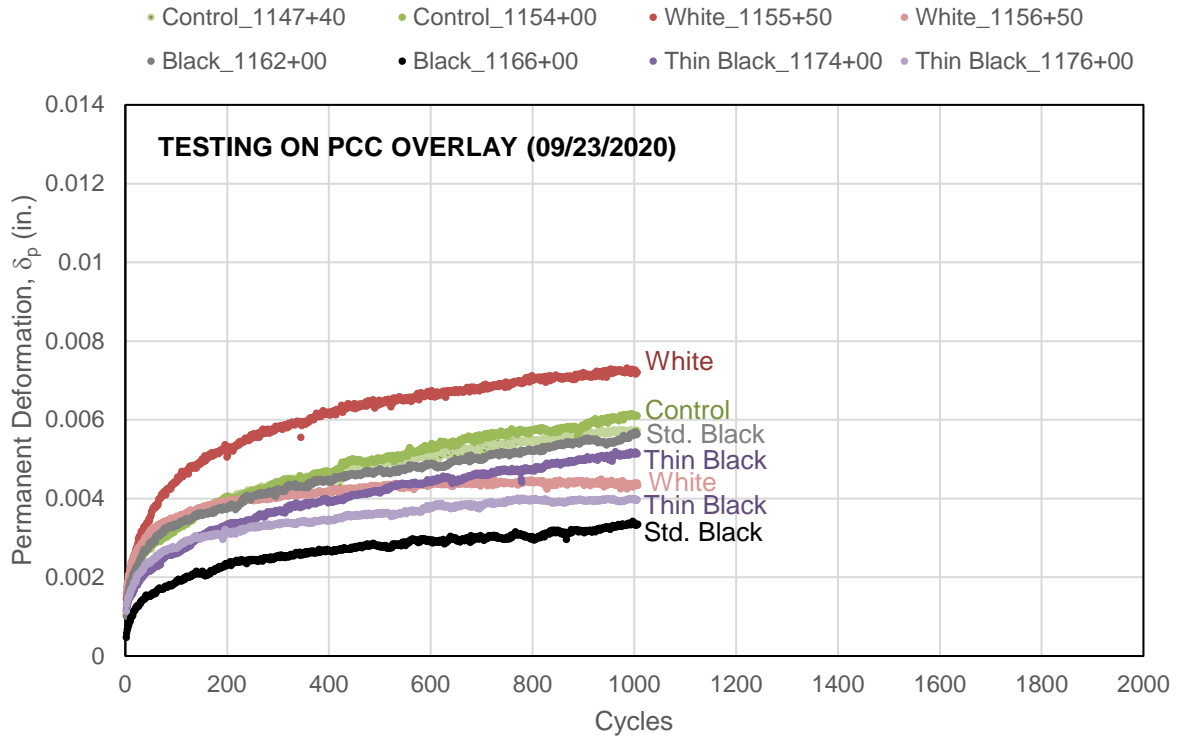
Figure 24. Comparison of δ_p results from cyclic APLTs performed on PCC overlay on September 23, 2020 (top) and September 1, 2021 (bottom)

Similarly, $M_{r\text{-comp}}$ values are compared in Figure 25.
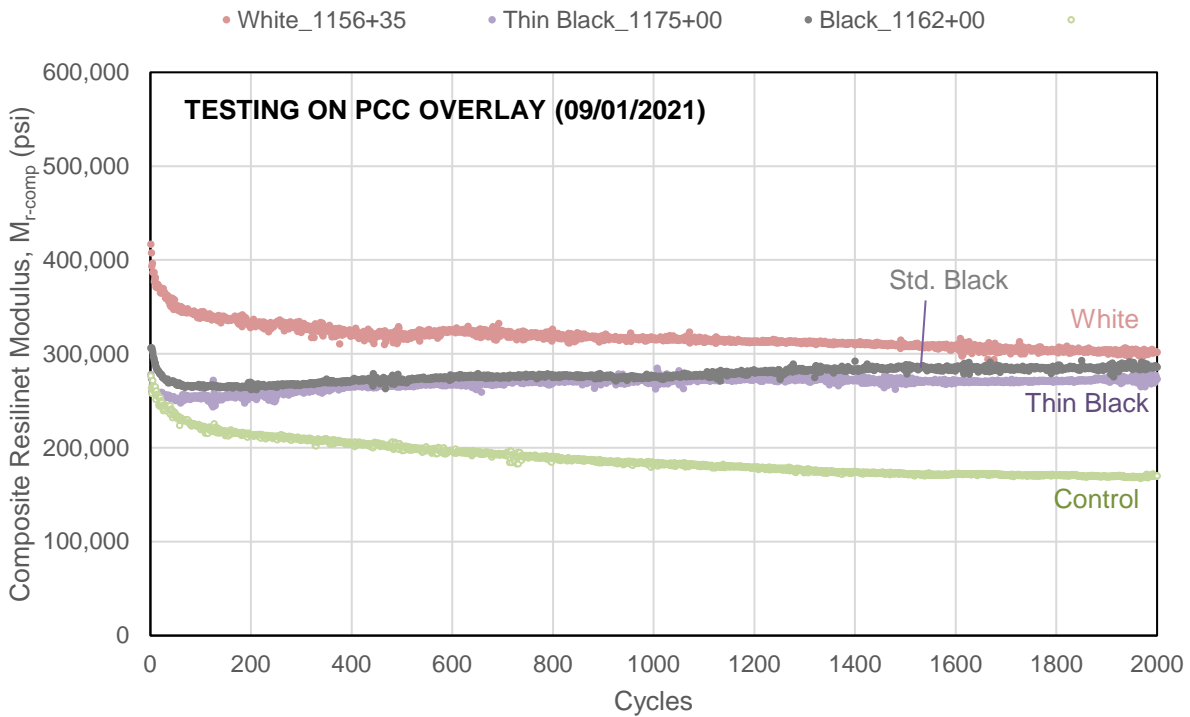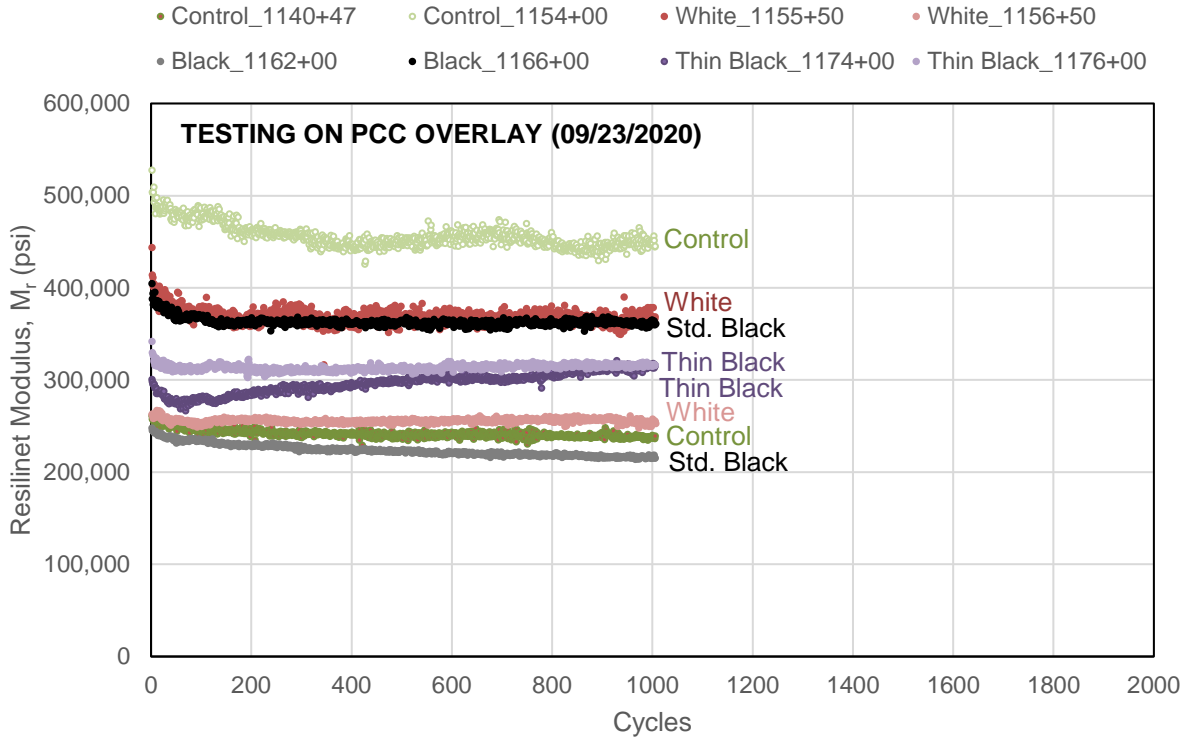
Figure 25. Comparison of M$_{r\text{-comp}}$ results from cyclic APLTs performed on PCC overlay on September 23, 2020 (top) and September 1, 2021 (bottom)

Figure26 compares the $M_{r\text{-comp}}$ and δ_p results from September 23, 2020 and September 1, 2021at the same or nearby test locations in each of the sections.
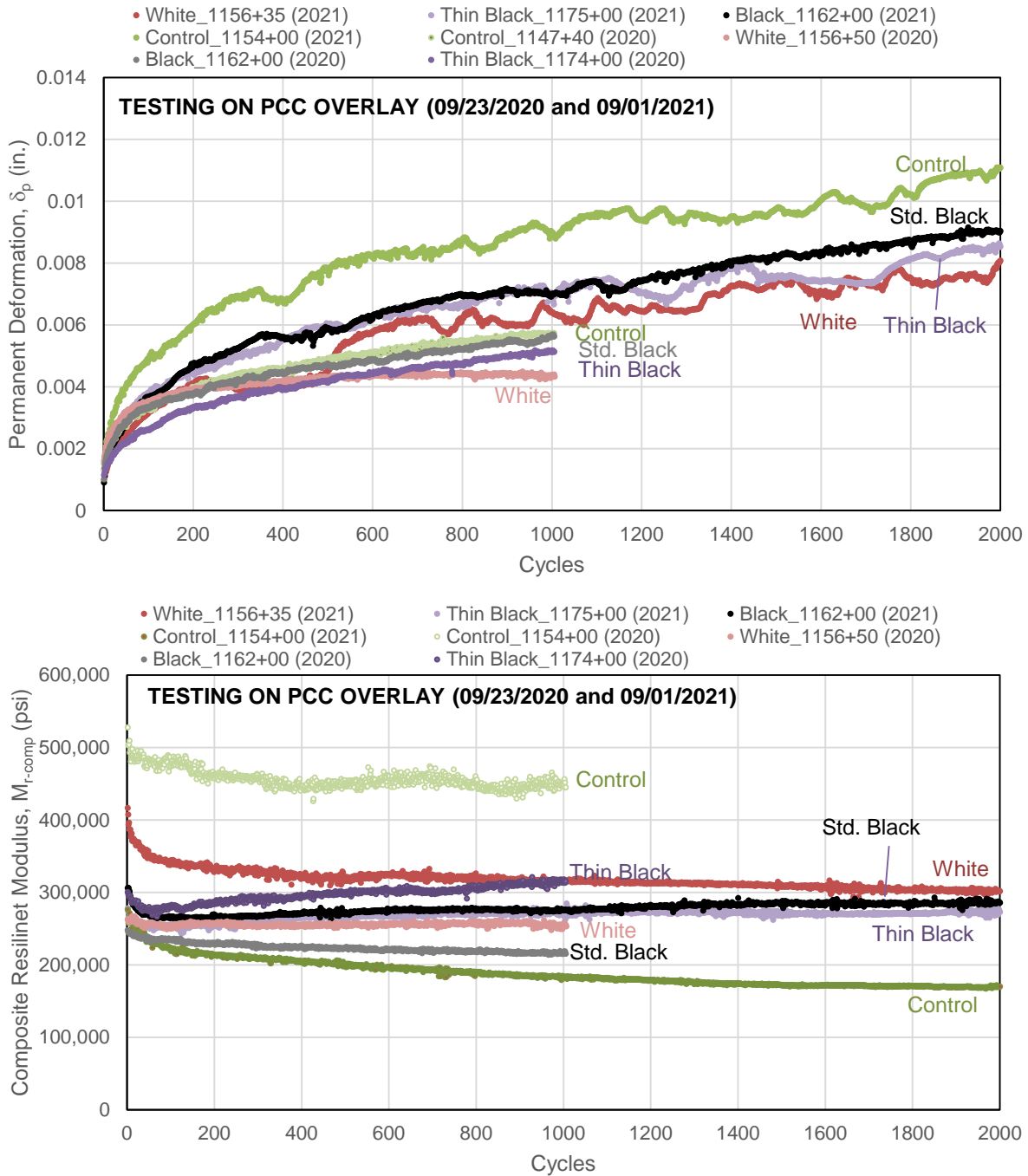
Figure 26. Comparison of cyclic APLTs performed on PCC overlay at or near same test loctations on September 23, 2020 and September 1, 2021 – δ_p (top) and $M_{r\text{-comp}}$ (bottom)

δ_p and $M_{r\text{-comp}}$ values are presented as bar charts in Figure 7, comparing test results on the existing ACC and on the PCC overlay on September 23, 2020 and September 1, 2021.
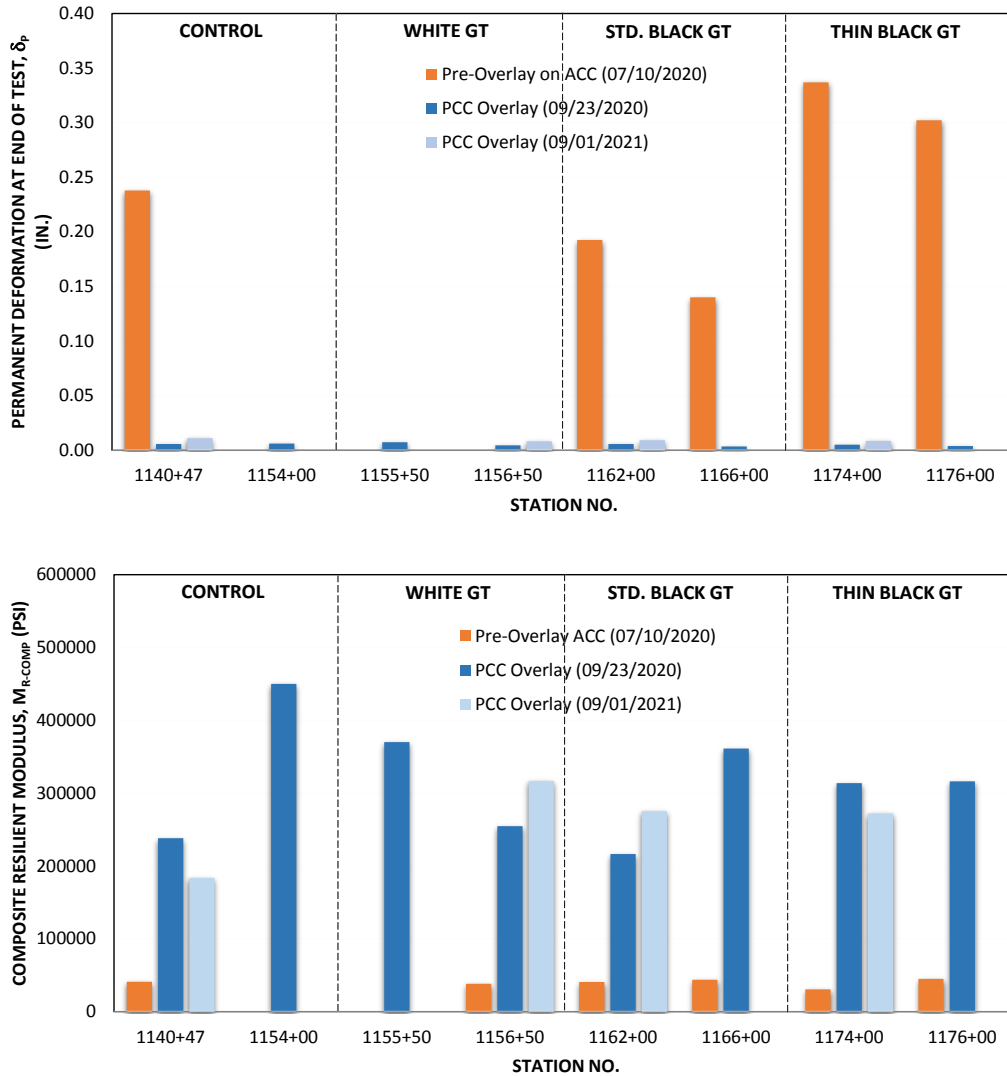
Figure 27. Comparison of cyclic APLT results – permanent deformation (δ_P) at end of test (top) and M$_{r\text{-comp}}$ (bottom)

The k-values calculated from the cyclic and static APLTs are summarized in Tables 6 and 7 from September 23, 2020 testing.

Back-calculated k-values are presented as bar charts in Figure 8, comparing results from September 23, 2020 and September 1, 2021.
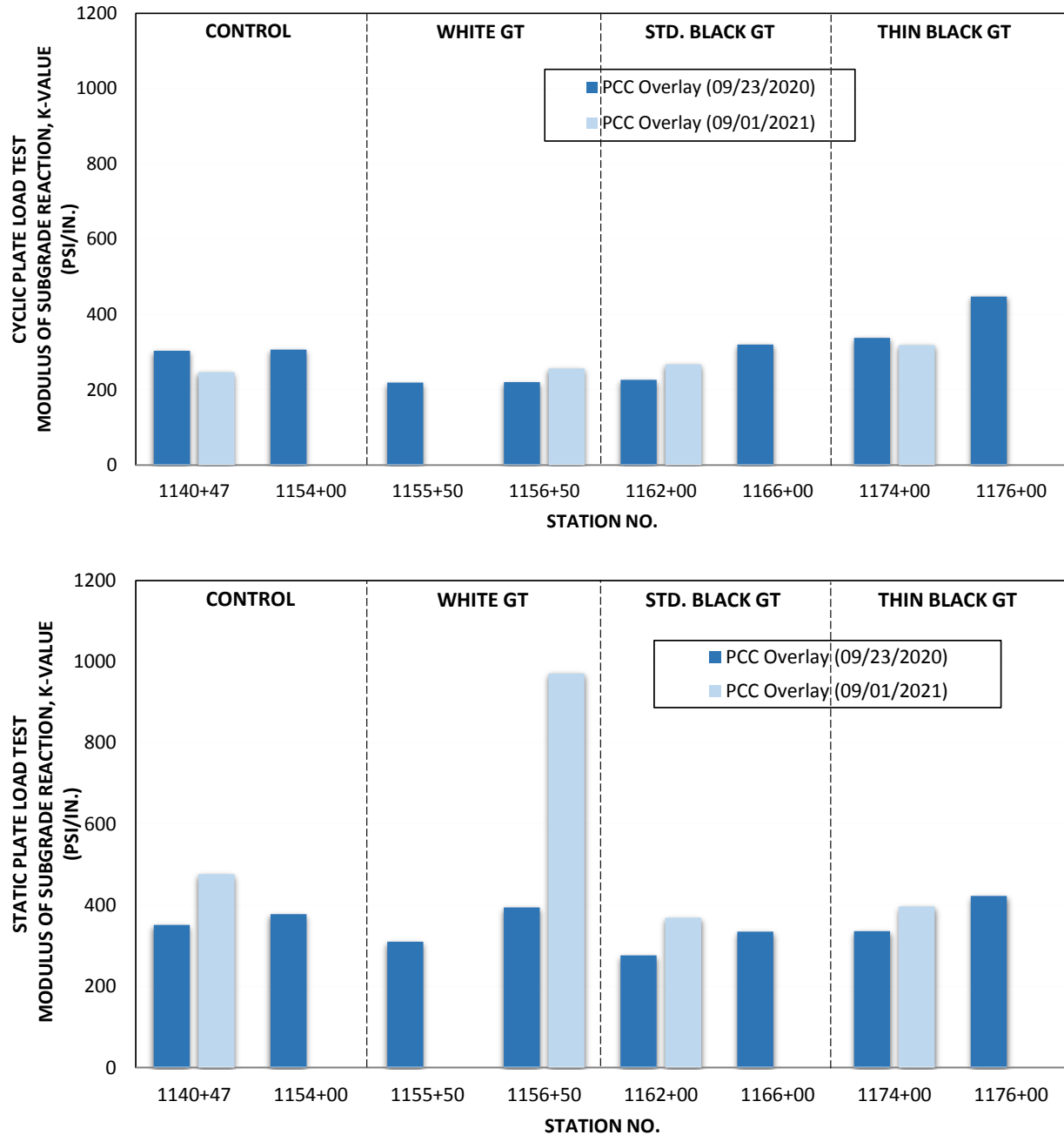
Figure 28. Comparison of backcalculated k-values from static (top) and cyclic (bottom) APLT results

The δ_p values at the end of 1,000 cycles on the PCC overlay on September 23, 2020 ranged between 0.003 (3 mils) and 0.007 in. (7 mils), at nominal cyclic stress = 90 psi. The M_{r-comp} values ranged between 216 ksi and 450 ksi, which represented about a 10-times increase in the modulus values comparing the original ACC pavement system and the new PCC overlay. The δ_p values at the end of 2,000 cycles on the PCC overlay on September 1, 2021 ranged between 0.008 (8 mils) and 0.011 in. (11 mils), at nominal cyclic stress = 90 psi. The M_{r-comp} values ranged between 184 and 317 ksi.

The δ_p values (at 1,000 cycles) in all the sections were higher on September 1, 2021 than on September 23, 2020 but still low (<0.05 in.). The $M_{r\text{-comp}}$ values decreased in the control section by 2.5 times. The $M_{r\text{-comp}}$ values in the geotextile sections were slightly lower based on the September 1, 2021 test results (white and standard black geotextile sections decreased 10% to 30%, respectively, and the $M_{r\text{-comp}}$ value in the thin black geotextile section decreased about 10%). Small variations (~0.001 in.) in the δ_p versus loading cycle curves for the September 1, 2021 results were due to vibrations and movements from traffic in the lane adjacent to the test setups, given the roadway needed to stay open to traffic.

Based on tests conducted on September 23, 2020, the back-calculated k-values from the cyclic APLTs ranged between 219 psi/in. and 447 psi/in., and the back-calculated k-values from the static APLTs ranged between 276 psi/in. and 423 psi/in. These k-values represented the support condition at the bottom of the PCC overlay. Based on the tests conducted on September 1, 2021, the back-calculated k-values from the cyclic APLTs ranged between 247 and 318 psi/in., and the back-calculated k-values from the static APLTs ranged between 369 and 971 psi/in.

The back-calculated modulus values of the PCC overlay (E_{PCC}) were summarized in the previous Tables 6 and 7. The E_{PCC} values at the test locations on September 23, 2020 varied between 2.9 million psi and 12.0 million psi based on the cyclic APLT results. The E_{PCC} values varied between 4.5 million psi and 22.6 million psi based on the static APLT results. The E_{PCC} values at the test locations on September 1, 2021 varied between 1.7 million psi and 6.0 million psi based on the cyclic APLT results. The E_{PCC} values varied between 3.1 million psi and 7.1 million psi based on the static APLT results.

The back-calculated k-value and E_{PCC} comparisons for the static and cyclic loading cases was the first of its kind for PCC overlays. The current AREA method of back calculation (AASHTO 1993) is based on a static loading case, but the calculation method is widely implemented for dynamic analysis by applying an empirical correction factor to determine a static k-value. This comparison of static and cyclic loading cases to calculate k-values warrants further detailed analysis and testing comparisons.

SUMMARY OF KEY FINDINGS AND RECOMMENDATIONS

This study provided on opportunity to assess the performance of a PCC overlay on Buchanan CR D-16 in Iowa that included various geotextile interlayers in comparison to a control section with no geotextile. The overlay was constructed on an existing 12 in. thick ACC pavement.

In this report, the results presented provide comparisons of modulus and deformation before and after the overlay and between different test sections. APLTs were performed and provided the data for the load-deformation performance analysis. The pavement sections were constructed in July 2020, and the cyclic and static APLTs were conducted on the existing ACC pavement at two different times, September 23, 2020 and September 1, 2021, after the PCC overlay was constructed. Cyclic APLTs included 1,000 to 2,000 cycles at one selected stress (90 to 100 psi) and static APLTs included an incremental static load test up to 120 psi.

The key findings from the testing and analysis are presented below. Recommendations are also provided for continued monitoring and field testing to assess longer term performance of the overall area of the roadway with and without the geotextile interlayer.

Key Findings

- The amount of energy stored and transferred into a concrete mixture from a geotextile is significantly lower than that from an asphalt layer.

- The composite modulus plots indicated that, even after the concrete started deflecting, the textile was still able to absorb some additional strain. Deflection of the geotextiles was ~0.05 in.

- The $M_{r\text{-comp}}$ values on the existing ACC pavement ranged from 27.7 ksi to 45.1 ksi based on 12 test locations. The $M_{r\text{-comp}}$ values increased in the first 10 to 20 cycles and then remained relatively constant up to 1,000 cycles. The δ_p values increased with the number of loading cycles up to 1,000 cycles following a power model trend. δ_p at the end of 1,000 cycles ranged between 0.19 in. (190 mils) and 0.34 in. (340 mils) at the test locations.

- The back-calculated ACC layer dynamic modulus (corrected for surface temperature to 72°F) at the test locations varied between 76.2 ksi and 140.9 ksi. $M_{r\text{-Base}}$ varied between 14.3 and 32.3 ksi, and $M_{r\text{-SG}}$ varied between 16.8 and 29.1 ksi. Results indicated that the $M_{r\text{-comp}}$ values strongly correlated to the E'_{AC}, $M_{r\text{-Base}}$, and $M_{r\text{-SG}}$ values.

- The δ_p values at the end of 1,000 cycles on the PCC overlay (per testing September 23, 2020) ranged between 0.003 (3 mils) and 0.007 in. (7 mils) at nominal cyclic stress = 90 psi. In comparison to the existing ACC pavement, the δ_p values on the PCC overlay decreased by about 50 times.

- The δ_p values at the end of 2,000 cycles on the PCC overlay (per testing September 1, 2021) ranged between 0.008 (8 mils) and 0.011 in. (11 mils) at nominal cyclic stress = 90 psi. The

δ_p values (at 1,000 cycles) in all the sections were low (<0.05 in.) but higher than initial testing on September 23, 2020.

- The $M_{r\text{-comp}}$ values ranged between 216 ksi and 450 ksi on the PCC overlay (per testing September 23, 2020), which represented about a 10-times increase in the modulus after placing the PCC overlay in comparison to that for the original ACC pavement. The $M_{r\text{-comp}}$ values ranged between 184 and 317 ksi on September 1, 2021. The $M_{r\text{-comp}}$ values decreased in the control section by 250%, while the $M_{r\text{-comp}}$ values increased nominally (10% to 30%) in the white and standard black geotextile sections, respectively. The $M_{r\text{-comp}}$ value in the thin black geotextile section decreased nominally (10% lower September 1, 2021 compared to September 23, 2020).

- The back-calculated k-value and E_{PCC} comparison for static and cyclic loading cases were presented in this report and was a first of its kind analysis. The current AREA method of back calculation (AASHTO 1993) is based on a static loading case, but the calculation method is widely implemented for dynamic analysis by applying an empirical correction factor to determine a static k-value. This comparison of static and cyclic loading cases to calculate k-values warrants further detailed analysis.

Recommendations

The results presented in this report represent a new method for in situ performance assessment of mechanistic properties of unbonded concrete overlays. Overall, the performance results are encouraging that geotextile interlayers provide suitable and improved performance.

Tests were performed shortly after construction and about one year after initial testing. The findings presented should be assessed as showing potential for performance differences but given a limited data set. The following additional testing and monitoring is recommended to provide a future statistically robust data set to further quantify the differences between interlayer materials.

Results from this study indicated that the structural capacity of the pavement reduced (as indicated with decreased $M_{r\text{-comp}}$ by 250% and increased δ_p by 80%) about one year after construction in the control section. In the sections with a geotextile interlayer, the $M_{r\text{-comp}}$ value increased slightly (10 to 30%) in two sections and decreased slightly (10%) in one section, while the δ_p values were low (<0.05 in.). It is recommended to monitor the changes in the load-deformation response of the pavement structure over time (3, 5, and 10 years after construction).

The ride quality of the test sections, i.e., international roughness index (IRI) and pavement condition index (PCI), with and without the geotextile fabric interlayers should also be documented annually.

Literature suggests that the geotextile interlayer provides an added benefit over the AC layer by providing enhanced drainage. Assessing drainage was not within the scope for the field testing but should be considered in future field studies. In situ drainage capacity of the interlayer can be achieved using the core hole permeameter (CHP) test device that was developed as part of a

previous Iowa Highway Research Board project (White et al. 2014). A 6 in. diameter core is required for the CHP test.

REFERENCES

American Association of State Highway and Transportation Officials, Washington, DC:

AASHTO. 2015. *Mechanistic-Empirical Pavement Design Guide: A Manual of Practice*, 2nd Edition.

AASHTO. 1986, 1993. *AASHTO Guide for Design of Pavement Structures*.

AASHTO T 307. 1999. *Standard Method of Test for Determining the Resilient Modulus of Soils and Aggregate Materials*.

AASHTO TP 62. 2007. *Standard Test Method for Determining Dynamic Modulus of Hot-Mix Asphalt Concrete Mixtures*.

AASHTO T 222-81. 2012. *Standard Method of Test for Nonrepetitive Static Plate Load Test of Soils and Flexible Pavement Components for Use in Evaluation and Design of Airport and Highway Pavements, Standard Specifications for Transportation Materials and Methods of Sampling and Testing*, 32nd edition.

AASHTO T 324-11. 2015. *Standard Test Method for Determining Dynamic Modulus of Hot-Mix Asphalt Concrete Mixtures*.

ASTM International, West Conshohocken, PA:

ASTM C469. *Standard Test Method for Static Modulus of Elasticity and Poisson's Ratio of Concrete in Compression.*

ASTM D6951-03. *Standard Test Method for Use of the Dynamic Cone Penetrometer in Shallow Pavement Applications*.

Author-Date Citations:

Appea, A. K. 2003. *Validation of FWD Testing Results at The Virginia Smart Road: Theoretically and by Instrument Responses*. PhD dissertation. Virginia Polytechnic Institute and State University, Blacksburg, VA.

Baltzer, S. and J. M. Jansen. 1994. Temperature Correction of Asphalt Moduli for FWD Measurements. *Proceeding of the 4th International Conference on Bearing Capacity of Roads and Airfields*, Minneapolis, MN.

Barker, W. R. and D. R. Alexander. 2012. *Determining the Effective Modulus of Subgrade Reaction for Design of Rigid Airfield Pavements Having Base Layers*. Final Report ERDC/GSL TR-12-20. U.S. Army Corps of Engineers, Washington, DC.

Bly, P., D. Tompkins, and L. Khazanovich. 2011. *Allowable Axle Loads on Pavements*. Minnesota Department of Transportation, St. Paul, MN.

Burwell, B. 2014. *Oklahoma's Use of Fabrics in Overlays and PCCP Design*. Presented at the 2014 North Carolina Concrete Pavement Conference, American Concrete Pavement Association – Southeast Chapter, October 28–29, Charlotte, NC.

Cackler, T., T. Burnham, and D. Harrington. 2018. *Performance Assessment of Nonwoven Geotextile Materials Used as the Separation Layer for Unbonded Concrete Overlays of Existing Concrete Pavements in the US*. National Concrete Pavement Technology Center, Iowa State University, Ames, IA. https://intrans.iastate.edu/app/uploads/2018/10/US_geotextile_performance_w_cvr.pdf.

Canestrari, F. and E. Santagata. 2005. Temperature Effects on the Shear Behavior of Tack Coat Emulsions Used in Flexible Pavements. *International Journal of Pavement Engineering,* Vol. 6, No. 1, pp. 39–46.

Chang, J. R., J. D. Lin, W. C. Chung, and D. H. Chen. 2002. Evaluating the Structural Strength of Flexible Pavements in Taiwan Using the Falling Weight Deflectometer. *International Journal of Pavement Engineering*, Vol. 3, No. 3, pp. 131–141.

Chen, D.-H., J. Bilyeu, H.-H. Lin, and M. Murphy. 2000. Temperature Correction on Falling Weight Deflectometer Measurements. *Transportation Research Record: Journal of the Transportation Research Board*, No. 1716, pp. 30–39.

Crovetti, J. A. 1994. *Evaluation of Jointed Concrete Pavement Systems Incorporating Open Graded Bases*. PhD dissertation. University of Illinois at Urbana-Champaign, IL.

FAA. 2007. *R&D Review – From Research to Results, Innovative Projects from the FAA Airport Technology R&D Program*. Issue 2. Federal Aviation Administration, Washington, DC.

Fick, G., J. Gross, M. B. Snyder, D. Harrington, J. Roesler, and T. Cackler. 2021. *Guide to Concrete Overlays*. Fourth edition. National Concrete Pavement Technology Center, Iowa State University, Ames, IA. https://intrans.iastate.edu/app/uploads/2021/11/guide_to_concrete_overlays_4th_Ed.pdf.

Hall, K., M. Darter, T. E. Hoerner, and L. Khazanovich. 1997. *LTPP Data Analysis Phase I: Validation of Guidelines for K-Value Selection and Concrete Pavement Performance Prediction*. FHWA-RD-96-198. Federal Highway Administration, McLean, VA.

Hall, K., D. Dawood, S. Vanikar, R. Tally, Jr., T. Cackler, A. Correa, P. Deem, J. Duit, G. Geary, A. Gisi, A. Hanna, S. Kosmatka, R. Rasmussen, S. Tayabji, and G. Voigt. 2007. *Long-Life Concrete Pavements in Europe and Canada*. FHWA-PL-07-027. Federal Highway Administration, Washington, DC.

Huang, Y. H. 2004. *Pavement Analysis and Design.* Second Edition. Pearson Education, Inc., Upper Saddle River, NJ.

Johnson, A. M. and R. L. Baus. 1992. Alternative Method for Temperature Correction of Backcalculated Equivalent Pavement Moduli. *Transportation Research Record: Journal of the Transportation Research Board*, No. 1355, pp. 75–81.

Kim, Y. R., B. O. Hibbs, and Y.-C. Lee. 1995. Temperature Correction of Deflections and Backcalculated Asphalt Concrete Moduli, *Transportation Research Record: Journal of the Transportation Research Board*, No. 1473, pp. 55-62.

Lederle, R. E., K. Hoegh, T. Burnham, and L. Khazanovich. 2013. *Drainage Capabilities of a Nonwoven Fabric Interlayer in an Unbonded Concrete Overlay*. 92nd Annual Transportation Research Board Meeting, January 13–17, Washington, DC.

Lukanen, E. O., R. N. Stubstad, and R. Briggs. 2000. *Temperature Predictions and Adjustment Factors for Asphalt Pavement*. FHWA-RD-98-085. Federal Highway Administration, McLean, VA.

Monismith C. L., N. Ogawa, and C. R. Freeme. 1975. Permanent Deformation Characteristics of Subgrade Soils Due to Repeated Loading. *Transportation Research Record: Journal of the Transportation Research Board*, No. 537, pp. 1–17.

PCS/Law Engineering. 1993. *SHRP-P-655: SHRP's Layer Moduli Backcalculation Procedure*. Strategic Highway Research Program, Washington, DC.

Rasmussen, R. O. and S. Garber. 2009. *Nonwoven Geotextile Interlayers for Separating Cementitious Pavement Layers: German Practice and U.S. Field Trials*. Federal Highway Administration. Washington DC.

Romanoschi, S. A. and J. B. Metcalf. 2003. Errors in Pavement Layer Moduli Backcalculation Due to Improper Modeling of Layer Interface Condition. *Proceedings of the 2003 Annual Transportation Research Board Conference,* Washington, DC.

Sholar, G. A., G. C. Page, J. A. Musselman, P. B. Upshaw, and H. Moseley. 2002. *Preliminary Investigation of a Test Method to Evaluate Bond Strength of Bituminous Tack Coats.* Florida Department of Transportation, Gainesville, FL.

Smith, K. D., J. E. Bruinsma, M. J. Wade, K. Chatti, J. M. Vandenbossche, and H. T. Yu. 2017. *Using Falling Weight Deflectometer Data with Mechanistic-Empirical Design and Analysis, Volume I: Final Report*. FHWA-HRT-16-009. Federal Highway Administration, McLean, VA.

Stubstad, R. N., S. Baltzer, S., E. O. Lukanen, and H. J. Ertman-Larsen. 1994. Prediction of AC Mat Temperature for Routine Load/Deflection Measurements. *Proceeding of the 4th International Conference on Bearing Capacity of Roads and Airfields*, Minneapolis, MN.

Tandon, V. and I. Deysarkar. 2005. Field Evaluation of Tack Coat Quality Measurement Equipment, *International Journal of Pavement Engineering*, Vol. 4, No. 1–2, pp. 25–37.

Ullidtz, P. 1987. *Pavement Analysis.* Elsevier, Amsterdam.

Ullidtz, P. and Peattie K. R. 1982. Programmable Calculators in the Assessment of Overlays and Maintenance Strategies. *Proceedings of the 5th International Conference on Structural Design of Asphalt Pavements – Volume I*, pp. 671–681, Delft, South Holland, the Netherlands.

U.S. Army Corps of Engineers. 1995. *Handbook for Concrete and Cement Standard Test Method for Determining the Modulus of Soil Reaction*. COE CRD-C 655-95. U.S. Army Corps of Engineers.

West, R. C., J. Zhang, and J. Moore. 2005. *Evaluation of Bond Strength Between Pavement Layers*. National Center for Asphalt Technology, Auburn University, AL.

Wiegand, P. D., J. K. Cable, T. Cackler, and D. Harrington, D. 2010. *Improving Concrete Overlay Construction*. National Concrete Pavement Technology Center, Iowa State University, Ames, IA. https://intrans.iastate.edu/app/uploads/2018/03/TR-600_report.pdf.

White, D. J. and P. Vennapusa. 2014. *Optimizing Pavement Base, Subbase, and Subgrade Layers for Cost and Performance of Local Roads*. National Concrete Pavement Technology Center, Iowa State University, Ames, IA. https://intrans.iastate.edu/app/uploads/2018/03/local_rd_pvmt_optimization_w_cvr.pdf.

White, D. J. and P. Taylor. 2018. *Automated Plate Load Testing on Concrete Pavement Overlays with Geotextile and Asphalt Interlayers: Poweshiek County Road V-18*. National Concrete Pavement Technology Center, Iowa State University, Ames, IA. https://intrans.iastate.edu/app/uploads/2018/04/Powashiek_CR_V-18_APL_testing_w_cvr.pdf.

National Concrete Pavement
Technology Center